THE BATHYMETRIC ZONATION AND COMMUNITY STRUCTURE OF DEEP-SEA MACROBENTHOS IN THE NORTHERN GULF OF MEXICO

A Thesis

by

CHIH-LIN WEI

Submitted to the Office of Graduate Studies of
Texas A& M University
in partial fulfillment of the requirements for the degree of

MASTER OF SCIENCE

December 2006

Major Subject: Oceanography

THE BATHYMETRIC ZONATION AND COMMUNITY STRUCTURE OF DEEP-SEA MACROBENTHOS IN THE NORTHERN GULF OF MEXICO

A Thesis

by

CHIH-LIN WEI

Submitted to the Office of Graduate Studies of
Texas A& M University
in partial fulfillment of the requirements for the degree of

MASTER OF SCIENCE

Approved by:

Chair of Committee, Gilbert T. Rowe
Committee Members, Jay R. Rooker
Daniel C. O. Thornton
Head of Department, Robert R. Stickney

December 2006

Major Subject: Oceanography

ABSTRACT

The Bathymetric Zonation and Community Structure of Deep-Sea Macrobenthos in the Northern Gulf of Mexico. (December 2006)

Chih-Lin Wei, B. S., National Chung-Hsing University

Chair of Advisory Committee: Dr. Gilbert T. Rowe

Macrobenthos of the deep, northern Gulf of Mexico have been sampled with large box cores along multiple cross-depth transects extending from depths of 200 m out to 3700 m. Four major depth zones have been identified based on the faunal similarities (β diversity) between geographic sites, with the two intermediate-depth zones being divided horizontally down the middle of the basin. The input of food resources appears to control the observed patterns. Each zone and sub-zone can be described by a characteristic animal density, biomass and biodiversity (α diversity). Highest densities and biomass occurred in two large submarine canyons, the Mississippi and De Soto Canyon, but the two habitats are markedly different. The α diversity displays an intermediate depth maximum. Species richness (γ diversity) is highest on east mid-slope, due, we suggest, to habitat complexity, but α diversity is lowest at the canyon head due to extreme dominance by amphipods. Small mean individual size and low densities encountered are a reflection of the meager surface water primary production, albeit with exceptional isolated habitats in which detrital material is concentrated, such as canyons on the upper continental slope.

DEDICATION

To my family

ACKNOWLEDGEMENTS

I would like to thank my committee chair, Dr. Gilbert T. Rowe, and my committee members, Dr. Jay R. Rooker and Dr. Daniel C. O. Thornton, for their guidance and support throughout my research. I also would like to thank Dr. Fain Hubbard for his patience and understanding of my everlasting questions on deep-sea invertebrate.

I would like to thank the members of the deep-sea biology laboratory for many hours of sample sorting, including Archie Ammons, Clifton Nunnally, Lindsey Loughry, Matt Ziegler, Min Chen, Xiaojia Chen, Yousra Soliman, and Dr. Yuning Wang. The macrofauna identifications were conducted by Dr. Amelie Scheltema, Dr. Fain Hubbard, Dr. George Wilson, Dr. Iorgu Petrescu, John Forster, Dr. Mary Wicksten, Roe Davenport, Min Chen, Yousra Soliman, and Dr. Yuning Wang. I also would like to thank Captain Dana Dyer and the crew of R/V Gyre for their assistance. This research was funded by the US Department of Interior, Minerals Management Service, Contract No 1435-01-99-CT-30991.

TABLE OF CONTENTS

LIST OF FIGURES

FIGURE Page

LIST OF TABLES

1. INTRODUCTION

The deep ocean was once thought to be a quiescent environment because of extreme pressure. At depth below the effect of seasonal change, deep-sea fauna was believed to be distributed continuously due to minimal change in the environment (Thomson, 1880). The concept of deep-sea zonation did not emerge until the complete results of the 'Challenger' Expedition had been published. In Murray's (1895) summary, he objected to Thomson's theory and suggested that distinct faunal assemblages were present on the shelf and abyss, as well as a zone of transition in between. This pioneering research led to recent interests of faunal zonation in the 20th century. In their early syntheses of deep-sea biology, Ekman (1953) and Menzies et al. (1973) advocated identifying a zonal boundary as the depth of maximum faunal change. However, this can be confused with the boundary between the faunal homogeneities or patterns of uniform change, where the faunal assemblage does not change across an environmental gradient (Carney et al., 1983). To imply that the deep-sea zonation is taking place continuously with depth or space, the "zonation" should be described as a non-repeating, sequential species replacement, in which all or some of the species have restricted ranges of distribution (Rex, 1981; Carney et al., 1983; Carney, 2005). The faunal boundary is better described as areas of slow faunal change bounded by areas of rapid faunal change across depths (Hecker, 1990; Gage and Tyler, 1991).

Previous studies of zonation in the deep sea have focused primarily on the general

---

This thesis follows the style of Deep-Sea Research

patterns of megafauna assemblages (Vinogradova, 1962; Rowe and Menzies, 1969; Grassle et al., 1975; Haedrich et al., 1975, 1980; Ohta, 1983; Hecker, 1990; Cartes and Carrassón, 2004) or distribution and abundance of individual taxa, such as fishes (Day and Pearcy, 1968; Stefanascu et al., 1993; Jacob et al., 1998; Moranta et al., 1998; Powell et al., 2003), decapod crustaceans (Cartes and Sardà, 1993), gastropods (Rex, 1977), echinoderms (Gage et al., 1984; Gage, 1986; Howell et al., 2002), and holothurians (Carney and Carey, 1976; Billett, 1991). Relative few studies have focused on the zonation of macrofauna (Rowe et al., 1982; Gage et al., 2000; Cartes et al., 2003; Olabarria, 2005). Most of the investigations described above have reported non-repeating, sequential patterns of species distributions in bands parallel to isobaths along the continental margin. Some authors have also suggested that the horizontal variation of faunal composition might be related to changes in physical or chemical conditions within geographical areas (Markle and Musick, 1974; Cutler, 1975; Hecker, 1990).

Carney et al. (1983) proposed three types of depth-related gradients causing zonation. The first is the gradient that is physiologically important to an animal, such as temperature (Rowe and Menzies, 1969; Haedrich et al., 1975), hydrostatic pressure (Siebenaller and Somero, 1978; Somero et al., 1983; Young and Tyler, 1993; Young et al., 1996), and dissolved oxygen concentration (Carney and Carey, 1976; Pearcy et al., 1982; Gage, 1986). However, the greatest variance in these factors only occurs within the top 1000m; therefore, it is unlikely that these physiological factors affect patterns of zonation at greater depths. The second is the resources that change relative composition with depth, such as sediment types (Rowe and Menzies, 1969; Day and Pearcy, 1968;

Haedrich et al., 1975). Since deep-sea infauna is mostly comprised of deposit feeders (Sanders and Hessler, 1969), animal composition and distribution may be linked to grain size (Gray, 1974) and sediment heterogeneity (Etter and Grassle, 1992). The third is a function of resources that change with depth, such as the decrease in available food (Cartes and Sardà, 1993) and increase in available space with depth (Carney et al., 1983). Several authors also suggested that topography and bottom currents may affect food supplies (Rowe and Menzies, 1969; Hecker, 1990; Rice et al., 1990; Tyler and Zibrowius, 1992) and larval dispersal (Rowe and Menzies, 1969; Cutler 1975; Grassle et al., 1979; Billett, 1991), which may lead to isolation and zonation on an evolutionary time scale. Rex (1981) proposed life history tactics (Sanders and Grassle 1971; Sanders 1977; Grassle et al. 1979), competition, and predation (Rex, 1977, 1981; Haedrich et al., 1980; Cartes and Sardà, 1993) as important biological parameters mediating the faunal composition; therefore, the zonal patterns can vary considerably among groups of taxa and different size categories (Rex 1981). In general, the causes of deep-sea zonation are elusive and patterns of zonation are likely due to both environmental heterogeneity and biological interactions.

Other depth related patterns, such as standing stocks and species diversity, have also been extensively discussed for the deep-sea environment. Macrofaunal stocks decrease exponentially with depth (Rowe and Menzel, 1971; Rowe et al., 1974; Rowe, 1983), but the overall level of stocks vary on different continental margins, depending on the surface production, width of the continental shelf, latitude (Rowe, 1983), and terrestrial runoff, while the rate of decreased stocks with depth is related to the quality

and quantity of particulate organic materials (POM) sinking to the bottom (Gage and Tyler, 1991). Since mid-water and benthic communities share the same food resources, the efficiency of consumption in water column will affect the benthic standing stocks. Rowe et al. (1974) suggested that macrofaunal stocks decay as an exponential function of depth, where the intercept of the stocks is associated with surface primary productivity, and the decay constant is related to the efficiency, both physically and trophically, that organic matter moves from surface to the seafloor.

High biodiversity in the deep sea is well documented (Hessler and Sanders, 1967). The species richness of macrobenthos is comparable to tropical shallow water (Sanders, 1968). Rex (1981) demonstrated a parabolic pattern of macrofauna diversity in the western North Atlantic, where the diversity had maximum value at intermediate depths and was depressed toward the shallow and abyssal depths. He also proposed Huston's (1979) dynamic equilibrium model to explain this pattern, in which nutrient fluxes control the population growth rate and the rate that a community approaches competitive equilibrium. The competitive exclusion by the dominant species could depress the species diversity, while the biotic and physical disturbance may prevent reaching competitive equilibrium and free up niches for the coexisting species; therefore, the increase in species diversity toward intermediate depths can be explained by the decreasing of food resources and competition with depth. The depression of diversity on the abyssal plain might be the result of energy constraints. However, very little is known about the variations of competition, predation, or the biotic and physical disturbances with depth in the deep sea; thus, the model is difficult to parameterize and still remains

theoretical. It should be noted that the parabolic diversity pattern is not universal in all taxa or geographic areas (Rex et al., 1997; Stuart et al., 2001). The boundary constraints, productivity gradients, sediment heterogeneity, oxygen availability, hydrodynamic regimes, and catastrophic events are included as factors that may alter diversity pattern (Levin et al., 2001).

Generally, biological diversity can be defined as "the variety and abundance of species in a defined unit of study" (Magurran, 2004), which can be partitioned into two components: species richness and species evenness (Simpson, 1949). To avoid confusion, we adapted Magurran's (2004) definitions to refer to "species richness measurement" as techniques that focus on estimating the numbers of species per specific numbers of individual or sample, "heterogeneity measurement" as techniques that focus on describing the variability in species abundance, and "species richness" exclusively as the full species list in a geographic unit. In this study, three levels of biological diversity were measured across space or depth. (1) α diversity is called within-habitat diversity, which is an appropriate measurement of number of species in a sample of standardize size. (2) β diversity is called between-habitat diversity, in which the degree of species turnover or compositional change is related to environment gradients. The faunal zonation can also be referred as β diversity. (3) λ diversity is called the landscape diversity and often refers to the total species richness or number within a large geographic region (Whittaker, 1960, 1972).

The Gulf of Mexico (GoM) is a semi-enclosed sea covering area of 1.5 million km^2 from tropical to subtropical climate with a maximum depth a little more than 3.7km

(Bryant et al., 1991). The continental margin of the GoM has one of the most complex physiography and bathymetry of the world's oceans. The sculpturing effects of salt and shale diapiric activities, as well as the slumping, debris flows, and turbidity currents on the slope, have created over ninety basins and seven submarine canyons (Rowe and Kennicutt, 2006). The world's third largest river, the Misssissippi, not only provides tremendous amounts of fresh water and nutrients but also contributes to the distinct features in the northeastern GoM, the Mississippi Canyon and Fan. The eastern part of GoM is dominated by the anticyclonic Loop Current, a branch of the Gulf Stream, which enters through the Yucatan Channel and exits through the Straits of Florida, bringing warm Caribbean water into the GoM (Jochens and DiMarco, In press). Large anticyclonic eddies detach from the Loop Current, as well as Rossby waves, propagate westward and southward. Below 1000m, strong currents have been observed in the eastern, central, western basin (Hamilton, 1990), and in the vicinity of Sigsbee Escarpment (Hamilton and Lugo-Fernandez, 2001).

Quantitative deep-sea sampling of the GoM began in the mid 1960s, but studies addressing faunal zonation patterns were limited. The most extensive sampling was the Northern Gulf of Mexico Continental Slope Study (NGoMCS) funded by the Minerals Management Service (MMS) in the 1980s. In NGoMCS study, Pequegnat et al. (1990) reported five megafaunal zones from cluster analysis, including a shelf/slope transition zone (118-475m), archibenthal zone (500-975m), upper abyssal zone (1000-2275m), messoabyssal zone (2300-3225m), and lower abyssal zone (3250-3850m). The most pronounced faunal turnover was reported at around 1000m. Powell et al. (2003)

suggested that fish fauna was zoned with depth and four faunal zones were identified on the outer shelf (188-216m), upper slope (315-785m), mid slope (689-1369m), and in the deep (1533-3075m). Baguley et al. (2006) identified 17 distinct zones from harpacticoid copepods on either east or west of longitude 91° W with little discernable association to depth. Carney (2005) reanalyzed the 185 most abundant macrofauna species from the NGoMCS study. That cluster analysis revealed a complicated picture in which 16 groups were organized more by region and year of sampling than by depth. From the previous studies in the GoM, the faunal zonation patterns seemed more pronounced in megafauna and fish than in the small size categories, such as macrofauna and meiofauna (Grassle et al., 1979; Gage and Tyler, 1991).

In this study, the North Gulf of Mexico Continental Slope Habitats and Benthic Ecology Study, or Deep Gulf of Mexico Benthos (DGoMB), systematic sampling was attempted to reexamine macrobenthos community composition and structure of the continental slope and abyssal plain in both vertical and horizontal scales. We hypothesized that (1) water depth is the single most important factor that shapes the macrofaunal community; (2) the input of nutrients from Mississippi River discharge might cause an east-west gradient in faunal composition and structure; (3) due to the funneling effect of Mississippi Canyon, macrofaunal species composition might be more similar to the shallow water assemblage in the northeastern GoM than in the northwestern GoM; (4) based on the previous studies, a non-repeating, sequential pattern of species replacement is expected to take place in the deep-sea northern GoM, in which the distinct faunal assemblages can be defined; and, finally, (5) if this zonal pattern does

exist, the standing stocks and diversity can be characterized and statistically separated into each distinct faunal assemblage. The community structure can be compared and contrasted with other oceanic regions with similar depth ranges and ocean climates. The pattern of faunal distribution can be compared with sedimentary processes and bottom chemical and physical properties to further elucidate possible causes of zonation, as well as provide a better understanding for the future management and conservation strategies of resource exploration in the deep-sea GoM.

2. MATERIALS AND METHODS

2.1. Site description

A total of 51 stations in the northern GoM was sampled from 2000 to 2002 during the DGoMB study (Figure 1, Table 1). The systematic sampling design included 7 transects with nested isobathic stations from depths of 200 to 3800m. Two transects, RW1-5 and W1-5, were sampled on the Texas slope. The other stations in this area included two historical sites, WC5 and WC12 (Pequegnat et al., 1990), basin sites (B1-3), non-basin sites (NB2-5), Bush Hill (BH), and Alaminos Canyon (AC1). The Sigsbee Escarpment is the southern boundary of the Texas-Louisiana Slope. Two stations, RW6 and W6, were sampled at the base of the escarpment as parts of the real west (RW) and west (W) transect, respectively. In the northeastern GoM, two transects were sampled on the Mississippi Canyon and Fan, with the central transect (C) on the west flank of the fan and the Mississippi Trough transect (MT) in the middle of the canyon. Transect S35-38 sampled the De Soto Canyon. Transect S39-44 sampled the West Florida Terrace, with S39-41 at the base of the Florida Escarpment and S42-44 above it. All the above sites were sampled in the year 2000. In ensuing years, the high productivity station (Hipro), Green Knoll Furrows (GKF), and five deep stations on the Sigsbee Abyssal plain (S1-5) were added. Details of the physiography and bathymetry of the Gulf of Mexico can be found in Bryant et al. (1991).

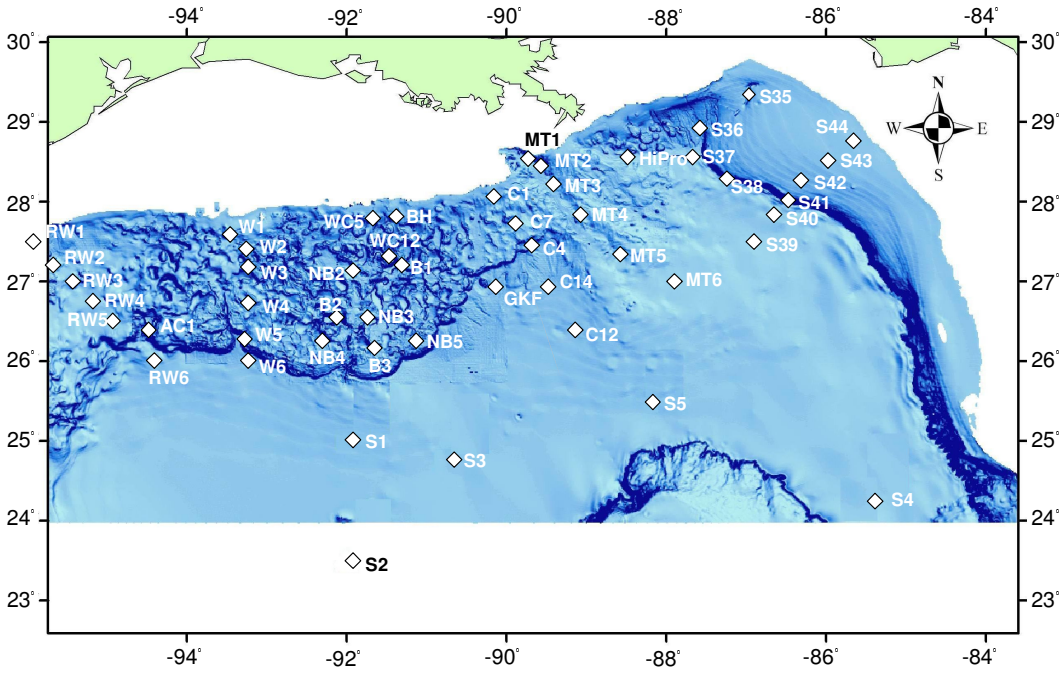

Fig. 1. Locations of the DGoMB stations (map by Dr. William Bryant)

Table 1. Location of the DGoMB stations

Station	Depth (m)	Lat	Lon	Numbers of cores in year		
				2000	2001	2002
AC1	2479	26.3903	-94.5598	5		
B1	2255	27.2024	-91.4042	5		
B2	2629	26.5511	-92.2197	5		
B3	2618	26.1649	-91.7343	5		
BH	542	27.7987	-91.4696		5	
C1	336	28.0597	-90.2493	5		
C7	1072	27.7306	-89.9815	3	5	
C4	1463	27.4551	-89.7732	5		
C14	2487	26.9315	-89.5699	5		
C12	2921	26.3781	-89.2408	5		
GKF	2465	26.9255	-90.2214		5	
HiPro	1572	28.5521	-88.5733		5	
MT1	481	28.5408	-89.8277	5	5	3
MT2	678	28.4502	-89.6722	4		
MT3	987	28.2196	-89.4944	5	5	
MT4	1401	27.8289	-89.1661	5		
MT5	2275	27.3325	-88.663	5		
MT6	2745	26.9998	-87.996	5	4	

Table 1. Continued

Station	Depth (m)	Lat	Lon	Numbers of cores in year		
				2000	2001	2002
NB2	1530	27.1346	-91.9996	5		
NB3	1875	26.5547	-91.8233	5		
NB4	2042	26.2501	-92.3935	5		
NB5	2063	26.25	-91.2112	5		
RW1	213	27.4998	-96.0018	5		
RW2	950	27.2058	-95.7468	5		
RW3	1329	27.0052	-95.4981	5		
RW4	1574	26.7502	-95.2484	5		
RW5	1620	26.5027	-95.0006	5		
RW6	3008	25.9992	-94.4945	5		
S1	3526	25.0034	-92.0016			2
S2	3732	23.5006	-92.0031			2
S3	3670	24.7554	-90.7549			2
S4	3409	24.2489	-85.4817			4
S5	3314	25.4901	-88.2632			2
S35	663	29.3336	-87.0502	5		
S36	1828	28.9188	-87.6713	5	5	2
S37	2384	28.555	-87.7633	5		
S38	2633	28.2771	-87.3314	5		
S44	213	28.7503	-85.7484	5		
S43	361	28.5023	-86.0791	5		
S42	767	28.2522	-86.4163	5	4	
S41	2979	28.0151	-86.5713	5	3	
S40	2954	27.8372	-86.7519	4		
S39	3001	27.4906	-86.9994	5		
W1	405	27.5779	-93.55	5		
W2	625	27.4136	-93.3396	4		
W3	863	27.1734	-93.3224	5		
W4	1452	26.7306	-93.32	5		
W5	2753	26.2698	-93.3574	4		
W6	3146	25.9956	-93.3121	5		
WC5	345	27.7795	-91.7645	5		
WC12	1166	27.3225	-91.553	4		

2.2. Sampling methodology

Samples were taken with a $0.2\,m^2$ version of the GOMEX box core (Boland and Rowe, 1991) aboard the R/V Gyre (formerly belonging to and operated by Texas A&M

University). At least 5 box cores were deployed at each station and overall 271 box cores were taken from the 51 locations, which equals over 46 m^2 of seafloor sampled. The sediments from the top 15cm of each box core were gently washed through 300μm sieve using the flotation method developed by Sanders et al. (1965). The material retained on the sieve was fixed in 10% buffered formalin diluted with filtered seawater. Samples were stained with 5% Rose Bengal for at least 24 hours, and then rinsed with freshwater. The stained samples were sorted into major taxonomic groups and transferred to 70% ethyl alcohol for permanent preservation. Six macrofauna taxa, including amphipods (Mr. John Forster and Ms. Yousra Soliman), aplacophorans (Dr. Amelie Scheltema), bivalves (Ms. Min Chen, Dr. Mary Wikksten, and Mr. Roe Daveuport) cumaceans (Dr. Iorgu Petrescu), isopods (Dr. George Wilson), and polychaetes (Dr. Fain Hubbard and Dr. Yuning Wang) were identified into species by the named taxonomists. Density was estimated according to "Macrobenthos Sensu Stricto" (excluding nematodes, copepods, and ostrocodes) (Sanders et al., 1965; Hessler and Jumars, 1974; Rowe, 1983; Gage and Tyler, 1991; Gage et al., 2002). The volumetric dimensions of individual animal were obtained from 3 sub-cores (12.4 cm i.d.) from box cores at C7, MT1, MT3, MT6, S36, S42, using an ocular micrometer (data derived from Nunnally, 2003). The biovolumes (mm^3) were then converted to wet weights (mg) using a factor of 1.1 for seawater density. In S1, S3, S4, and S5, the preserved wet weights of macrofauna taxa were measured from a total of 6 box core replicates (data derived from Dr. Elva Escobar Briones of the Universidad Nacional Autónoma de México). Wet weights were then converted to carbon weight using the conversion factors determined by Rowe (1983) for

each major taxonomic group.

Environmental variables were measured along with the biological samples in the course of DGoMB study. Sediment properties, including grain size (% sand, % silt, % clay), total organic nitrogen (org-N %), total polyunclear aromatic hydrocarbon excluding perylene (PAH), trace metals, particulate organic carbon (POC), dissolved organic carbon (DOC), ammonium ($NH4^+$), urea, and nitrate ($NO3^-$), were obtained from 5 sub cores (6.5 cm i.d.) in the five separate box cores at each site.

The primary production was estimated using the mean bi-weekly (SeaWifs) chlorophyll concentration from 1998-2000 (Biggs et al., 2006, in press). The algorithm was derived from depth-integrated production estimated from a compilation of 24 hour incubation in the Celtic Sea (Behrenteld et al., 1998; Joint and Groom, 2000). The algorithm is: $PP = 676.083 * C_K^{0.563}$ where PP is primary production (mg $C/m^2/d$) and C_K is the estimated chlorophyll concentration (mg/ m^3). SeaWifs data were not available at the five deepest stations (S1-5) sampled in 2002, and thus the estimation (44 g $C/m^2/yr$) of Biggs et al. (2006) for the deepwater GoM was used as a proxy. Since export fluxes of primary production is a function of depth below the euphotic zone (Suess, 1980; Betzer et al., 1984; Martin et al., 1987; Berger et al., 1988; Christensen, 2000), the downward flux of POC was estimated by the equation: $J(z) = 0.409 * Z^{-0.628} * PP^{1.41}$ (Betzer et al., 1984; Berger et al., 1988), where J(z) (mg $C/m^2/yr$) is the export fluxes transported to the depth of Z (m) and PP is the primary production (mg $C/m^2/yr$).

The remaining variables, including salinity, dissolve oxygen (DO), and water

temperature (Temp), were measured using the CTD/rosettes. The environmental data and complete list of macrobenthos taxa and species are archived in the Dept. of Marine Biology, Texas A & M at Galveston, (Gilbert T. Rowe, the DGoMB Program Manager, as well as at the National Oceanographic Data Center (NODC) and the Ocean Biogeographic Information System (OBIS).

2.3. Data analyses

2.3.1. Univariate analyses

The α diversity was estimated using the method developed by Sanders (1968) and modified by Hurlbert (1971) to give an absolute measure of species richness, rarefaction index: $E(S_n) = \sum_{i=1}^{S}\left[1 - \frac{(N - N_i)!(N - n)!}{(N - N_i - n)!N!}\right]$, where $E(S_n)$ is the expected number of species in a sample of n individuals randomly selected from an assemblage containing N individuals and S species; N_i is the number of individuals in the *i*th species. Rarefaction is a technique to measure species richness independent of sample size. Although the assumption of each individual arriving independently in the sample is unrealistic and the expected number of species for the smaller sample size is constantly overestimated (Clarke and Warwick 2001), we prefer this technique due to our balanced sampling design and consistent collecting techniques (GOMEX box core), as well as its easy interpretation, robustness, and widely use in deep-sea research. The heterogeneity

component of α diversity was measured using Simpson's index, which is the probability of randomly choosing two individuals from the assemblage belonging to the same species (Simpson, 1949). In Simpson's index (λ') $= \sum_{i=1}^{S}\left[\frac{n_i(n_i-1)}{N(N-1)}\right]$, where n_i = the number of individuals in the *i*th species; and N = the total number of individuals. Simpson's index is one of the most meaningful and robust diversity measures. This nonparametric index makes no assumptions about species abundance distribution and provides a good diversity estimate at small sample size (Magurran, 2004). The most abundant species are heavily weighted so the diversity decreases as λ' increases. In order to be comparable with richness measures, its complement, 1- λ', was used to represent the species evenness. The evenness index ranges between 0 and 1, where 0 indicates that every individual belongs to the same species and 1 indicates that every individual belongs to a different species in the assemblage; therefore, 0 represents the lowest evenness and 1 represents the highest evenness.

β diversity was calculated using Bray-Curtis dissimilarity (Bray and Curtis, 1957). The dissimilarity between sample j and k is $\delta_{jk} = 100\left\{\frac{\sum_{i=1}^{n}\left|y_{ij}-y_{ik}\right|}{\sum_{i=1}^{n}\left(y_{ij}+y_{ik}\right)}\right\}$, where y_{ij} and y_{ik} are the abundance of the i th species in the j and k samples, respectively. Since the difference of abundance between the most dominant and rare species was as high as three orders of magnitude, the mean species abundance for each station was forth root-transformed to down-weigh the importance of dominant species. The matrix derived from the β diversities of every pair of stations was also later used to compute hierarchical clustering and non-metric multiple dimensional scaling (MDS).

The simplest estimate of γ diversity is the total number of observed species. However, the "true" γ diversity is usually underestimated, but to sample the entire inventory is also practically impossible in the deep sea. Hence, we used nonparametric estimators in which no species abundance model is required to pre-fit the data and the species accumulation curve is based on the underlying distribution. Theoretically, the curve will approach the asymptote when the species richness is reached, such that no additional species will be encountered when more samples are taken. The shape of the curve is also greatly affected by when and how many species are added in the accumulation curve. To produce a smooth line, the observed inventory was randomly added into the assemblage and the whole procedure was repeated 50 times to calculate the mean value, as well as plot the accumulated species against the sample size. Due to the difference of taxonomic efforts (the number of box core replicates being identified) between taxa (Table 2), incidence-based estimators were chosen to estimate γ diversity, including Choa2 (Chao, 1984 and 1987), ICE (Chao et al., 2000; Chazdon et al., 1998), and Jacknife2 (Burnham and Overton, 1978, 1979; Smith and van Belle, 1984; Palmer, 1991).

Other univariate procedures, such as correlation analysis and regression analysis, were conducted to examine the relationship between such community structure characteristics as abundance, α diversity, and β diversity with depth. Analysis of covariance (ANCOVA) with depth as the covariate was used to test that the animal density was not different among canyon and non-canon transects. One way analysis of variance (ANOVA) was carried out to test that the community characteristics, such as

density, biomass, E(S_n), and λ', were not different among the faunal zones defined by multivariate procedures. The treatment levels (faunal zones) were compared by Bonferroni (the observations are homogenous) and Dunnett's T3 tests (the observations are not homogenous). The homogeneity was confirmed by Levine's test.

Table 2. Number of box core replicates, species and specimens were identified in each taxa.

Taxa	Replicates	Species	Specimens
Aplacophoran	52	24	294
Bivalve	144	94	3645
Cumacean	128	120	877
Amphipod	173	121	10000
Isopod	151	136	2136
Polychaete	78	462	15228

2.3.2. Multivariate analyses

Species by station information was converted to Bray-Curtis similarity (1- δ_{ij}) and then subjected to cluster analysis (group-average linkage). At the same time, a similarity profile test (SIMPROF; Clarke and Gorley, 2006) was performed to test the null hypothesis that a specific subset of samples do not differ from each other in the multivariate structure. To conduct this test, the first step was generating an "observed" similarity profile in which all resemblances (Bray-Curtis similarities) in this subset of samples were ranked on the x-axis, while the similarity values were plotted on the y-axis;

then, an "expected" similarity profile was simulated by randomly rearranging the entry labels (species name) in the same subset of samples for 1000 times and plotting the mean values against the ranks. This "expected" profile represented a set of non-structural samples where all species were randomly rearranged. The sum of the absolute distances (π) between the "observed" and "expected" profile was the test statistic under the null hypothesis. Second, a further 999 simulated profiles (not including the "observed" one) were generated by permuting the sample labels (station names) and π was computed between each of these and the "expected" profile. If the real π was larger than any 949 out of 999 simulated π, the significant conclusion ($P<0.05$) can be made that the structure is present in the subset of samples. The same procedure was carried out on every branch of the dendrogram until significant evidence of structure was supported. This significance was a prerequisite for defining each faunal zone.

Another permutation-based procedure, ANOSIM, was performed to test the null hypothesis that there is no difference among the pre-defined groups of multivariate data. The R statistic (between -1 and 1) is a comparative measure of the degree of group separation: $R = \frac{\overline{r_B} - \overline{r_W}}{1/2\,M}$, where $\overline{r_W}$ is the average of all rank similarities among stations within groups; $\overline{r_B}$ is the average of rank similarities arising from all pairs of stations between groups; M = n(n-1)/2 and n is total number of stations under consideration. Thus, the higher R value indicates that stations within groups are more similar to each other than any station from different groups. The null distribution of R was calculated from random reshuffling the sample labels (station names). If 95% of this distribution

was smaller than the observed R, the null hypothesis would be rejected. Once the alternative hypothesis was accepted, pairwise tests were carried out based on Bonferroni correction to avoid a Type 1 error with a significance level of 0.05/n, where n was the numbers of pairwise comparisons.

Non-metric multiple dimensional scaling (MDS) was conducted on the same matrix of Bray-Curtis similarities to aid in the interpretations of the cluster analysis. The stress value is crucial for interpreting the MDS plot. The higher the stress the lower the accuracy of station relationships is represented by MDS; therefore, only MDS plot with a stress value$\leq$ 1.5 was used for describing the relationship of the sites (Clarke and Warwick, 2001). The average similarities within and between faunal zones were broken down by the similarity percentage routine (SIMPER) to the percent contribution of each species. The species which contributed the most within the zone and species which discriminate one zone from another were examined as characteristics of faunal zones.

Nearly a hundred environmental variables were measured in the course of the study. However, only data with few missing values (<10 sites) and not highly auto-correlated (Pearson's correlation, $\rho<0.9$) were retained for analysis. Based on these criteria, 22 trace metals and 13 sediment/bottom water properties were considered as useful measurements. Only 12 trace metals (As, Pb, Ti, Sb, Hg, Cd, Ag, Sr, Ca, Cu, Mn, and Ba) and 9 sediment/bottom water properties (% sand, PAH, % Org-N, dissolve oxygen, export POC flux, temperature, POC, DOC, and %Silt) were selected as non auto-correlated variables (Figure 2 a, b). The environmental data were logarithm transformed before analysis to approximate the parametric assumption and to emphasize

measurements of high and low values. The 12 trace metals were further reduced using Principal Component Analysis (PCA) into a new, smaller set of orthogonal dimensions with minimum loss of the information. The new dimension was defined by a linear combination of original variables, called principal components (PC). The first 2 PC explained 88.7% of the variation of the original data set, and so a new subset of trace metals (Ca, Mn, Pb, and Sr) was selected from the highest positive and negative loadings in the first 2 PC (Table 3). The new subset of trace metals plus the 9 sediment/ bottom water properties were then normalized, and the Euclidean distance, $d_{jk} = \sqrt{\sum_{i=1}^{p} (y_{ij} - y_{ik})^2}$, where the distance between station j and k is the root of sum of squared difference for the i th variable, was computed. These Euclidean distances were used as a proxy for macrofauna habitats to link with the species abundance information (the Bray-Curtis similarities). RELATE and BIOENV procedures were conducted to give the Spearman's rank correlation coefficient between these two matrices, as well as find the best subset of environmental variables giving the highest correlation.

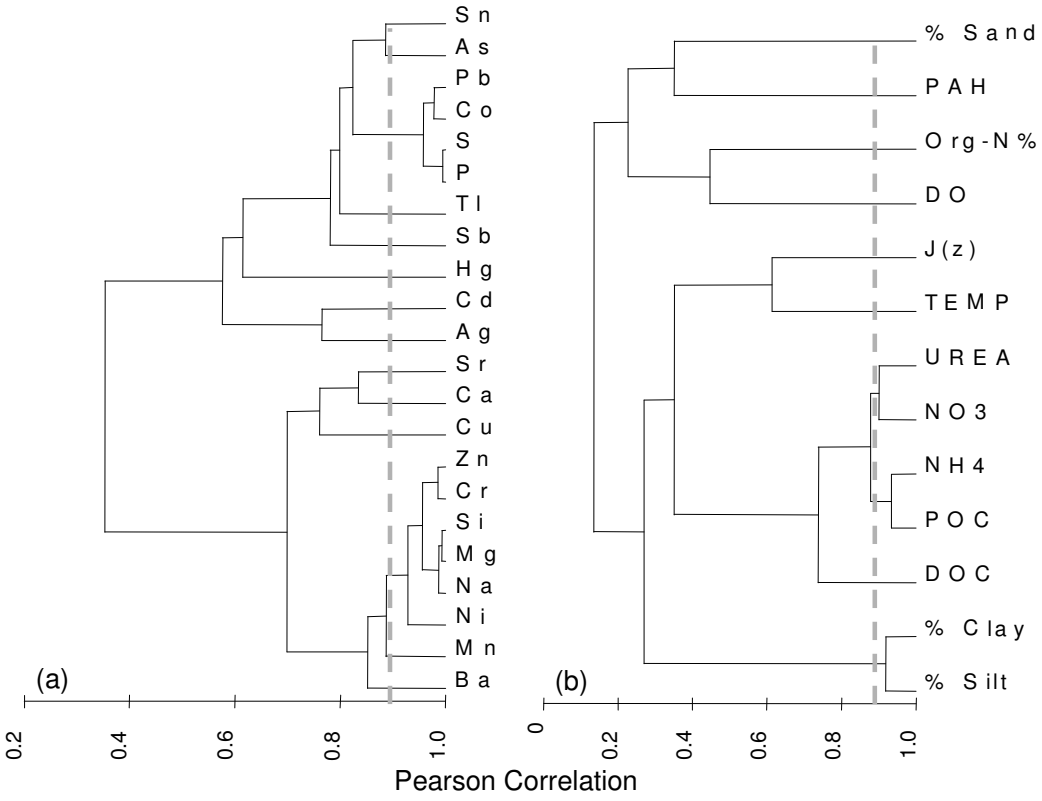

Fig 2. Dendrogram for the environmental variables. Group-linkage cluster analysis based on log transformed data and Pearson's correlation coefficient for (a) trace metals and (b) sediment/bottom water properties. The dotted lines represent the Pearson's correlation (ρ) =0.9. Note: J(z) is the export POC flux.

Table 3. Variable loads for trace metal PCA

Variable	PC1	PC2	PC3	PC4	PC5
Ag	0.004	0.009	-0.017	0.012	-0.011
As	0.113	0.457	-0.256	-0.278	-0.423
Ba	0.357	0.317	0.401	0.763	-0.071
Ca	**0.668**	-0.296	-0.538	0.107	0.275
Cd	0.011	0.025	-0.032	-0.023	0.011
Cu	0.198	-0.094	0.214	-0.142	-0.622
Hg	0.002	0.008	-0.002	-0.01	-0.016
Mn	**0.449**	0.344	0.452	-0.531	0.411
Pb	0.151	**0.482**	-0.445	0.061	-0.188
Sb	0.028	0.118	-0.002	-0.043	0.081
Sr	0.386	**-0.471**	0.179	-0.139	-0.378
Tl	0.025	0.082	-0.06	-0.029	0.002

Several software packages were used in data analyses. Correlation analysis, regression analysis, ANCOVA, ANOVA, and PCA are available in SPSS 13.0 (SPSS Inc., 2004). Rarefaction, Simpson's index, Bray-Curtis similarity, Euclidean distance, cluster analysis, MDS, SIMPROF, SIMPER, RELATE, BIOENVE, and ANOSIM procedures are available in PRIMER-E V6 (Primer Int., 2006). Species richness estimators, such as Choa2, ICE, and Jacknife2, are available in EstimateS 7.5 (http://purl.oclc.org/estimates). Figures and tables were generated using Microsoft Excel (Microsoft Int., 2003)

3. RESULTS

3.1. Patterns of faunal zonation

A total of 147,270 specimens was colleted and sorted into 36 macrofaunal taxa (Figure 3). Six of them, in 32,180 specimens, including amphipods, aplacophrans, bivalves, cumaceans, isopods, and polychaetes, were identified to 957 species and used to represent the total benthic macrofauna species composition. Hierarchical cluster analysis and SIMPROF revealed 13 significant groups (Figure 4, $P<0.05$), which can be categorized as 6 faunal zones (zone 1, 2W, 2E, 3W, 3E, 4) and 2 independent locations (GKF and WC5). Zone 1, 2 (including 2W and 2E), 3 (including 3W and 3E), and 4 were separated at the 25% similarity level; zone 2W and 2E were separated at the 30% similarity level; and Zone 3W and 3E were separated at the 29% similarity level. Due to the low faunal similarities with other stations (20.1-22.6%), the independent stations were not included in any faunal zone. The MDS plot (Figure 5, stress = 0.17) showed clear but uninterrupted distribution of faunal zones along the depth gradient. The negative direction of the x axis follows the shallow toward deep faunal zones. The y axis separates Zone 2E from 2W and Zone 3E form 3W. Generally, Zone 2E, 3E, and the east side of Zone 4 (S39, S40, and S4) were more close to Zone 1 than their western counterparts, indicating that the species composition of the east faunal zones, or the east side of zone 4, was shifted to more resemble Zone 1. Based on the results of cluster analysis and MDS, a map of deep-sea macrofaunal zones in the northern GoM was

generated (Figure 6). Due to the high stress value of the MDS plot (Figure 4, stress =0.17), separate MDS plots for faunal zones (Figure 7) were carried out to describe the structure in more detail. The significant faunal groups from the dendrogram (Figure 4) were superimposed to these plots.

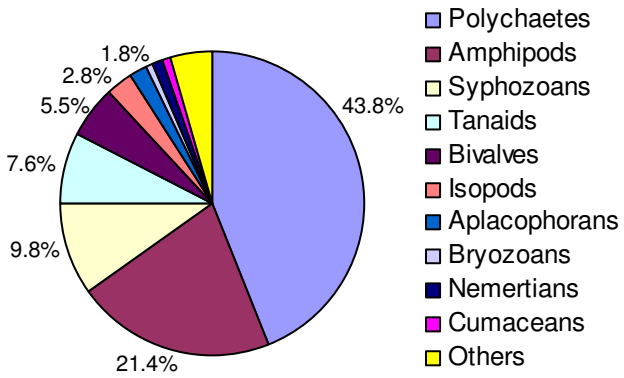

Fig. 3. Relative abundance of macrofauna taxa.

Zone 1 extended from 213m to 1572m, including the upper Texas-Louisiana Slope (RW1, W1, and BH), west flank of the upper Mississippi Fan (C1), the head of Mississippi Canyon (MT1, MT2), Hipro, and upper West Florida Terrace (S43, S44). The deepest site in the west side of Zone 1 was BH at 542m. In the east side, the deepest site was Hipro at 1572m, suggesting that Zone 1 extended deeper in the northeastern than in the northwestern GoM. Three significant groups were identified at 27% similarity (Figure 7a, stress = 0.12). RW1, S44, W1, C1, and S43 extended from 213m to 405m; MT1 and MT2 encompassed 481 to 678m; BH and Hipro were at 542 and 1572m, respectively, implying the separation of canyon sites from non-canyon sites and the 2 deepest sites in the east and west from other relative shallower sites.

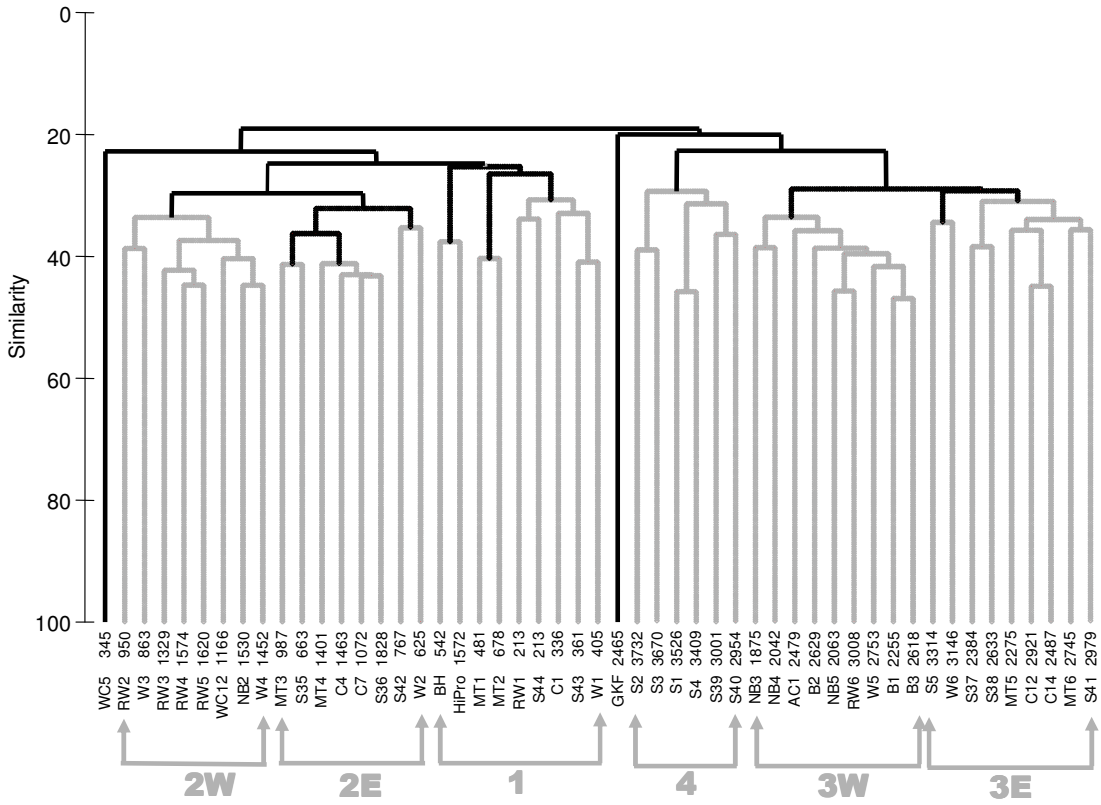

Fig. 4. Dendrogram for species abundance data. Group average-linkage cluster analysis for 4th root transformed species abundance data based on Bray-Curtis similarity. X axis represents the sampling depth (m), station names, and faunal zones. Y axis represents the Bray-Curtis similarity (%). Thick lines indicate significant evidence of structure (SIMPROF test, $P<0.05$) Thin lines indicate no evidence of structure.

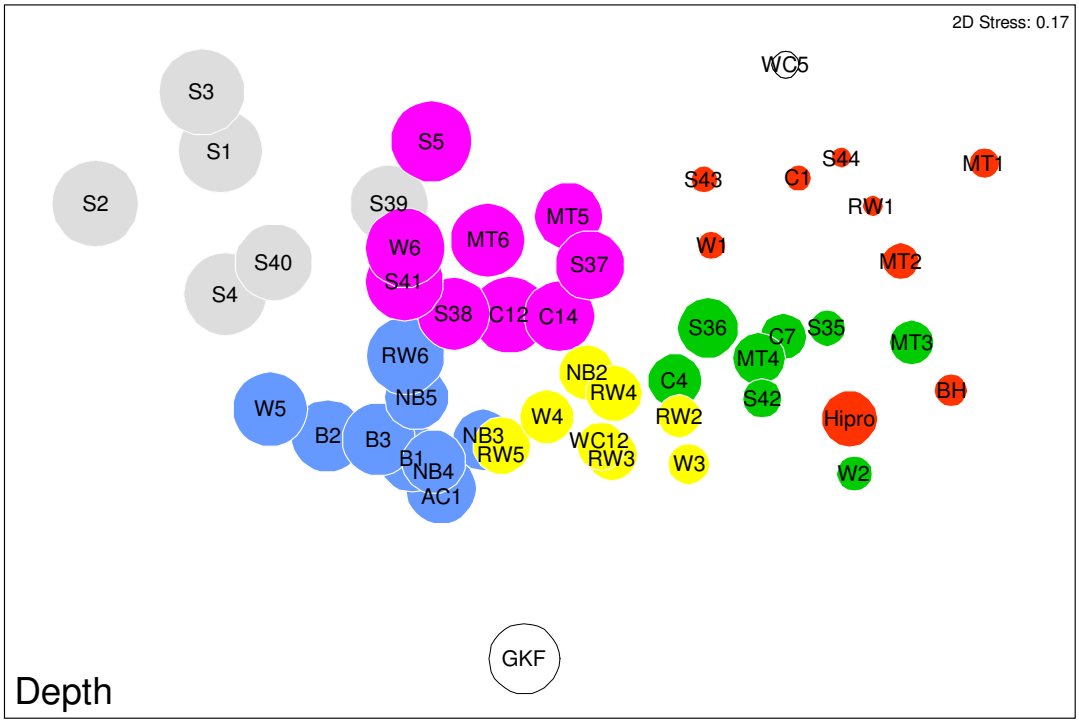

Fig. 5. Non-metric MDS plot for species abundance data. The analysis is based on 4th root transformed data and Bray-Curtis similarity. Bubble size equals to relative depths and color schemes represent different faunal zones. Note: WC5 and GKF are independent stations not included in any faunal zones.

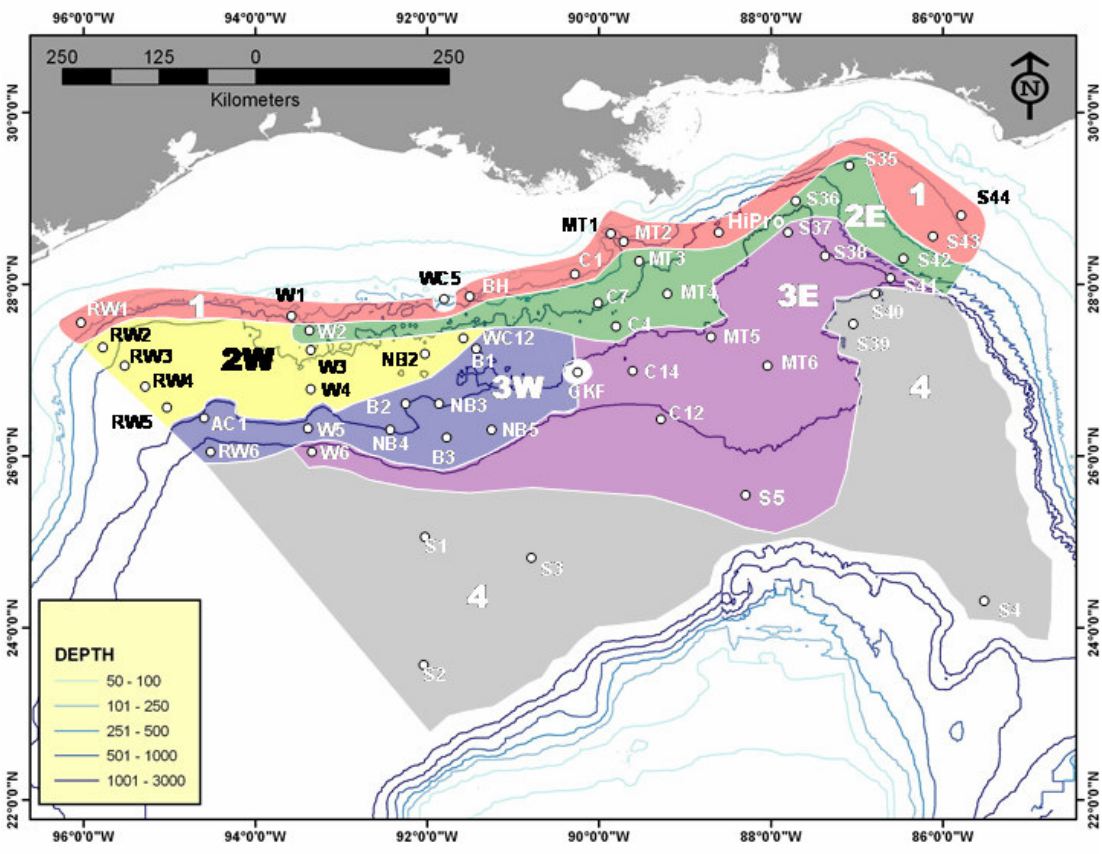

Fig. 6. Locations of faunal zones. The color schemes represent the different faunal zones. Note: WC5 and GKF are not included in any faunal zone.

Zone 2W extended from 863m to 1620 m, covering the mid Texas-Louisiana Slope with no significant internal structure (Figure 7b, stress = 0.07). Zone 2E extended from 625m to1828m, covering one station on the mid Texas-Louisiana Slope (W2), the west flank of the Mississippi Fan (C7, C4), the mid Mississippi Canyon (MT3, MT4), the head of De Soto Canyon (S35, S36), and the mid West Florida Terrace (S42). Three significant groups were identified in this zone (Figure 7c, stress = 0.04). Sites further away to the west and east from the Mississippi and De Soto Canyon (W2, S42) were

separated from sites close to the canyons at 35% similarity. Within those close canyon sites, two significant groups were separated at 40% similarity. MT3 and S35 were shallower at 663-987m; C4, C7, MT4, and S36 were deeper at 1072-1828m.

Zone 3W extended from 1875m to 3008 m and covered the most complex bathymetric features in northern GoM, including the Alaminos Canyon (AC1), basins sites(B1-2), non-basin sites (W5, NB3-5), and the base of the Sigsbee Escarpment (RW6). However, there was no indication that the same bathymetric features tended to group together (Figure 7d, stress = 0.12). Zone 3E included the west flank of the lower Mississippi Fan (C14, C12), the lower Mississippi Canyon (MT5, MT6), the lower De Soto Canyon (S37, S38), the lower West Florida Terrace (S41), the deep Mississippi Fan (S5), and one station at the base of the Sigsbee Escarpment (W6). Two significant groups were identified at 30% similarity (Figure 5e, stress = 0.15), separating the deeper W6 and S5 (3146-3314m) from other shallower sites (2275-2979m).

Zone 4 extended from 2954m to 3732m, covering the Sigsbee Abyssal Plain (S1-3), Florida Abyssal Plain (S4), and the base of the Florida Escarpment (S39, S40), with no significant internal structure (Figure 7f, stress = 0.03).

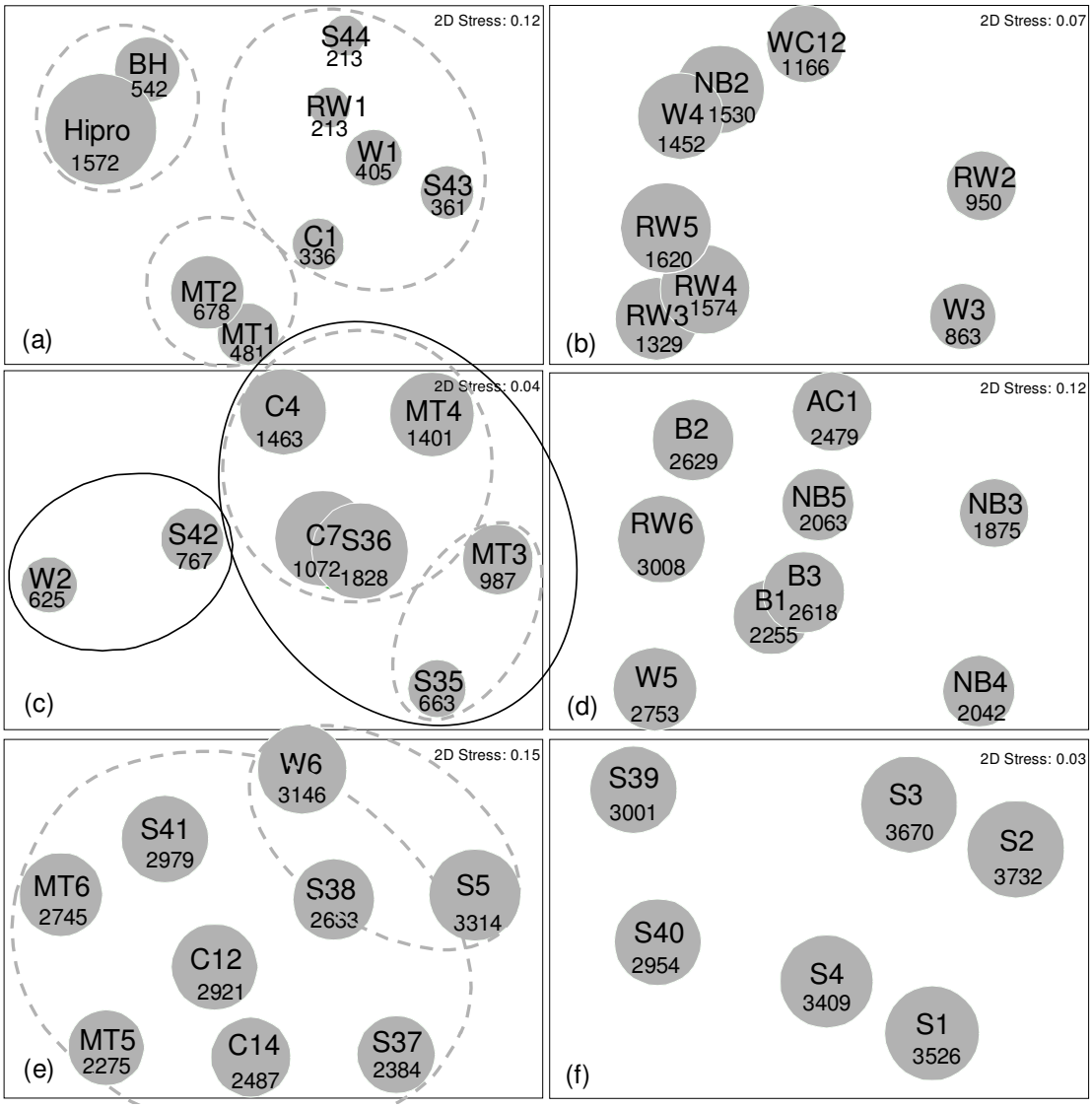

Fig. 7. Non-metric MDS plots for individual faunal zone. The analyses are based on 4th root tansformed data and Bray-Curtis similarity. Similarities are superimposed from hierarchical cluster analysis. Bubble size equals to relative depths within the faunal zone. (a) Zone 1: The dotted line is 27% similarity level. (b) Zone 2W. (c) Zone 2E: The dotted line is 35% and the solid line is 40% similarity level. (d) Zone 3W. (e) Zone 3E: The dotted line is 30% similarity level. (f) Zone 4.

3.1.1 Species contribution

The species contribution is usually compared by the relative abundance of species in the assemblage. However, at a large spatial scale, the most abundant species might be patchily distributed and absent in the majority of the area, and so it is not adequate for representing the species composition. The similarity breakdown to percent contribution of species (SIMPER) is a more objective method to find the most important species. The 5 species contributing the most to each faunal zone are shown in Table 4 based on SIMPER and Table 5 based on abundance. In Zone 1, the five species who accounted for 53.9 % of abundance contributed only a total of 5% to the average similarity. For example, the most abundant species amphipod *Ampelisca mississipina* occurred in Zone 1, 2W, 2E, and 3. Most records were in Zone 1 including RW1, C1, MT1, and S44. Relative few records were in Zone 2W (W3), 2E (S35, S42), and 3W (AC1). However, 99% of the specimens (15,851 individuals/m^2) were found at MT1, suggesting a very patchy distribution. In other faunal zones, the species who contributed the most to the average similarities and to the abundance were largely repeated. Between Tables 4 and 5, 4 species from Zone 2W, 2 species from Zone 2E, 4 species from Zone 3W, 4 species from Zone 3E, and 3 species from Zone 4 were repeated; thus, the dominant species were more evenly distributed in Zone 2W, 2E, 3W, 3E, and 4. On the other hand, some species had high contributions in more than one faunal zone (Table 4). Polychaete *Tharyx marioni* made a high contribution to Zone 1, 2W, and 3E; Bivalve *Heterodonta sp. B* contributed largely to Zone 3W, 3E, and 4; Polychaete *Aricidea suecia* made a high

contribution to Zone 1, 2W, and 2E. Two polychaetes (*Levinsenia uncinata*, *Paraonella monilaris*) were the important species in the most faunal zones, with the former contributing to Zone 1, 2W, 2E, and 3W and latter to Zone 2W, 3W, 3E, and 4. These species can be considered "the indicator species" contributing the faunal zonation.

SIMPER was also performed to breakdown the average dissimilarity between independent stations and their adjacent faunal zones (Table 6). The five most important species contributed 9.7% and 7.7% of the average dissimilarity between Zone 3W to GKF and Zone 3E to GKF, respectively. The bivalve Heterodonta species contributed extensively to the average similarity in Zone 3W and 3E, but were absent in GKF. These species made high contribution to the faunal difference between GKF and the two adjacent faunal zones. The rest of the species on the list of GKF were mostly broad-range species and did not occur either in Zone 3W or 3E, suggesting the species in GKF were some degree different from in Zone 3W and 3E. Between Zone 1 and WC5, most species that had high contribution to the dissimilarities were more abundant in WC5 than in Zone 1. The species abundances in Table 6 were the sum of the standardized abundance for 1 box core per site and there were 9 stations in zone 1; therefore, the abundance differences might be greater than it appeared on the table and had substantial effects on the dissimilarity.

Table 4. Five species contributing the most to the average similarity within faunal zones. Abundance (Abund.) is the sum of the animal numbers in the faunal zone that each station within zone was standardized to 1 box core.

Zone	Taxa	Species	Range	Abund.	Contrib.%	Cum.%
1	POL	*Tharyx marioni*	1,2W,2E,3W,3E,4	75	4.1	4.1
	POL	*Aricidea simplex*	1,2W,2E,3W,3E	78	3.7	7.8
	POL	*Levinsenia gracilis*	1,2W,2E,3E	38	3.3	11.1
	POL	*Levinsenia uncinata*	1,2W,2E,3W,3E,4	27	3.3	14.4
	POL	*Aricidea suecica*	1,2W,2E,3W,3E	88	2.8	17.2
2W	POL	*Paraonella monilaris*	1,2W,2E,3W,3E,4	50	4.1	4.1
	POL	*Levinsenia uncinata*	1,2W,2E,3W,3E,4	35	4	8.1
	POL	*Tharyx marioni*	1,2W,2E,3W,3E,4	59	3.6	11.7
	POL	*Aricidea suecica*	1,2W,2E,3W,3E	27	3.6	15.2
	POL	*Tachytrypane sp. A*	1,2W,2E,3W,3E,4	20	3.3	18.5
2E	POL	*Aricidea suecica*	1,2W,2E,3W,3E	54	2.2	2.2
	POL	*Exogone sp. A*	1,2W,2E,3W,3E	30	1.9	4.1
	POL	*Levinsenia uncinata*	1,2W,2E,3W,3E,4	31	1.8	5.9
	POL	*Paralacydonia paradoxa*	1,2W,2E,3W,3E	44	1.6	9.1
	POL	*Tharyx annulosus*	1,2W,2E,3W,3E,4	45	1.5	10.6
3W	BIV	*Heterodonta sp. C*	1,2W,2E,3W,3E,4	17	6.2	6.2
	BIV	*Heterodonta sp. B*	1,2W,2E,3W,3E,4	27	6.2	12.4
	POL	*Tachytrypane sp. A*	1,2W,2E,3W,3E,4	19	5.9	18.3
	POL	*Levinsenia uncinata*	1,2W,2E,3W,3E,4	30	4.8	23.1
	POL	*Paraonella monilaris*	1,2W,2E,3W,3E,4	26	4.1	27.2
3E	POL	*Paraonella monilaris*	1,2W,2E,3W,3E,4	96	6.7	6.7
	POL	*Tharyx marioni*	1,2W,2E,3W,3E,4	36	5.2	11.9
	BIV	*Heterodonta sp. B*	1,2W,2E,3W,3E,4	32	5.2	17.1
	BIV	*Heterodonta sp. C*	1,2W,2E,3W,3E,4	49	4.3	21.4
	POL	*Tachytrypane sp. A*	1,2W,2E,3W,3E,4	15	4.2	25.6
4	BIV	*Dacrydium vitreum*	1,3W,3E,4	9	11.6	11.6
	BIV	*Heterodonta sp. B*	1,2W,2E,3W,3E,4	7	11.3	22.9
	BIV	*Vesicomya vesica*	1,2W,2E,3W,3E,4	5	8.1	40.6
	POL	*Paraonella monilaris*	1,2W,2E,3W,3E,4	13	7.7	48.2
	ISO	*Macrostylis 519*	2W,3W,3E,4	6	7.4	55.6

Table 5. Five species contributing the most to the abundance within faunal zones. Abundance (Abund.) is the sum of the animal numbers in the faunal zone that each station within zone was standardized to 1 box core.

Zone	Taxa	Species	Range	Abund.	Contrib%	Cum.%
1	AMP	*Ampelisca mississippina*	1,2W,2E,3W	2744	44.9	44.9
	POL	*Litocorsa antennata*	1,2E,3E	232	3.8	48.7
	BIV	*Heterodonta sp. A*	1,2W,2E,3W,3E,4	139	2.3	50.9
	POL	*Prionospio cirrifera*	1,2E,3E	92	1.5	52.4
	POL	*Aricidea suecica*	1,2W,2E,3W,3E	88	1.4	53.9
2W	POL	*Tharyx marioni*	1,2W,2E,3W,3E,4	59	5.7	5.7
	POL	*Paraonella monilaris*	1,2W,2E,3W,3E,4	50	4.8	10.5
	POL	*Levinsenia uncinata*	1,2W,2E,3W,3E,4	35	3.4	13.9
	POL	*Macrochaeta clavicornis*	1,2W,2E,3W,3E,4	27	2.6	16.5
	POL	*Aricidea suecica*	1,2W,2E,3W,3E	27	2.6	19.2
2E	POL	*Litocorsa antennata*	1,2E,3E	85	3.5	3.5
	POL	*Aricidea suecica*	1,2W,2E,3W,3E	54	2.2	5.8
	BIV	*Heterodonta sp. D*	1,2W,2E,3W,3E	46	1.9	7.7
	POL	*Tharyx marioni*	1,2W,2E,3W,3E,4	45	1.9	9.5
	POL	*Paralacydonia paradoxa*	1,2W,2E,3W,3E	44	1.8	11.3
3W	POL	*Levinsenia uncinata*	1,2W,2E,3W,3E,4	30	5.5	5.5
	BIV	*Heterodonta sp. B*	1,2W,2E,3W,3E,4	27	4.9	10.4
	POL	*Paraonella monilaris*	1,2W,2E,3W,3E,4	26	4.8	15.2
	POL	*Tachytrypane sp. A*	1,2W,2E,3W,3E,4	19	3.5	18.6
	ISO	*Macrostylis 256*	1,2W,2E,3W,3E	18	3.3	21.9
3E	POL	*Paraonella monilaris*	1,2W,2E,3W,3E,4	96	10.2	10.2
	BIV	*Heterodonta sp. C*	1,2W,2E,3W,3E,4	49	5.2	15.4
	POL	*Tharyx marioni*	1,2W,2E,3W,3E,4	36	3.8	19.2
	BIV	*Heterodonta sp. B*	1,2W,2E,3W,3E,4	32	3.4	22.6
	ISO	*Macrostylis 519*	2W,3W,3E,4	26	2.8	25.4
4	POL	*Paraonella monilaris*	1,2W,2E,3W,3E,4	13	6.7	6.7
	POL	*Sigambra tentaculata*	1,2W,2E,3E,4	11	5.7	12.4
	BIV	*Dacrydium vitreum*	1,3W,3E,4	9	4.5	16.9
	POL	*Tharyx marioni*	1,2W,2E,3W,3E,4	7	3.6	20.5
	BIV	*Heterodonta sp. B*	1,2W,2E,3W,3E,4	7	3.6	24.1

Table 6. Five species contributing the most to the average dissimilarity between zone 3 to GKF and zone 1 to WC5. Abundance (Abund.) is the sum of the animal numbers in the faunal zone that each station within zone was standardized to 1 box core.

Taxa	Species	Range	Abund.	Abund.	Contrib%	Cum.%
			Zone 3W	GKF		
POL	*Fauveliopsis sp. A*	1,2W,2E,3E,4	0	3	2.1	2.1
BIV	*Heterodonta sp. B*	1,2W,2E,3W,3E,4	27	0	2.0	4.0
POL	*Leitoscoloplos sp.*	1,2W,2E	0	2	1.9	5.9
POL	*Sthenelais sp. A*	1,2W,2E,3E	0	2	1.9	7.8
CUM	*Leucon n. sp. 5*	2E,3E	0	2	1.9	9.7
			Zone 3E	GKF		
BIV	*Heterodonta sp. B*	1,2W,2E,3W,3E,4	32	0	1.6	1.6
BIV	*Heterodonta sp. C*	1,2W,2E,3W,3E,4	49	0	1.6	3.2
AMP	*Lysianassidae undet.*	1,2W,2E,3W,4	0	2	1.5	4.7
POL	*Leitoscoloplos sp.*	1,2W,2E	0	2	1.5	6.2
POL	*Exogone longicirrus*	1,2W,2E,3W,3E	22	4	1.5	7.7
			Zone 1	WC5		
POL	*Prionospio cristata*	1,2E,3W	10	302	1.9	1.9
POL	*Prionospio heterobranchia*	1,2W,2E	17	24	1.0	2.9
POL	*Gymnonereis sp.*	1,2W,2E,3E	1	13	0.9	3.7
POL	*Aricidea simplex*	1,2W,2E,3W,3E	78	0	0.8	4.5
POL	*Paleanotus sp. A*	WC5	0	5	0.8	5.3

3.1.2. Taxon contribution

In the analysis of species contributions (Table 4), polychaetes species were the most important taxon; however, the importance of bivalve species seems to increase from Zone 3W and 3E toward Zone 4. This trend of increasing importance became more

obvious when the species contributions were summed to taxon contributions in each faunal zone (Figure 8). The contribution of polychaete species was greater than any other taxa in Zone 1, 2W, 2E, 3W, and 3E; nevertheless, it decreased toward the deeper faunal zones. Eventually, the importance of bivalve species exceeded the polychaete species in Zone 4 and contributed 50% of average faunal similarity. Beside the polychaete and bivalve species that together contributed 73-81% of the average similarities in each zone, isopods were the third most important taxon with the contribution increasing slightly across Zone 1 to Zone 4. The overall pattern of faunal zonation was controlled by polychaete, bivalve, and isopod species and revealed a depth-dependent variation.

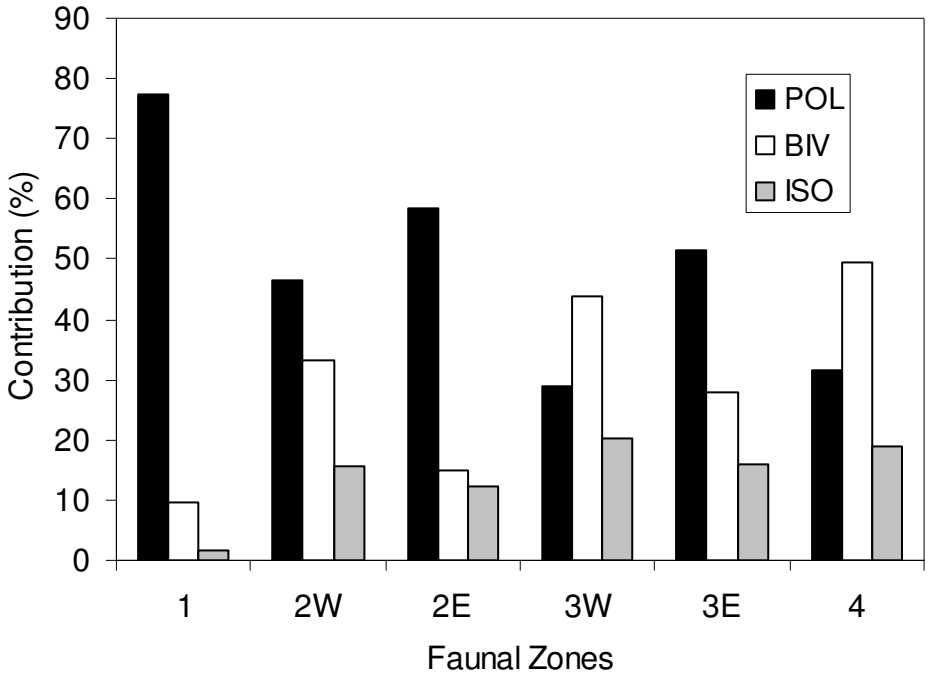

Figure 8: Contributions of polychaetes, bivalves, and isopods to the average Bray-Curtis similarity within each faunal zone.

3.1.3 Species co-existing ranges

The species were categorized based on the distribution among the specific combination of faunal zones. The co-existing species were grouped together and the numbers of co-existing ranges represented the species richness within the zone. Here I contrasted three different ranges of species distribution, including the stenozonal species of each zone, the euryzonal species that co-occurred throughout all zones, and the slope species that co-occurred in Zone 1, 2W, 2E, 3W, and 3E (Figure 9). Zone 1 and 2E had the most stenozonal species and the fewest euryzonal species. On the other hand, Zone 3W and 4 had the most euryzonal species and fewest stenozonal species. In addition, there were 39 slope species, contributing 12% to 20% species in Zone 2W, 3W, and 3E. The combinations of the two broadest ranges were accounted for 24% to 40% of species in Zone 2W, 3W, 3E, and 4, suggesting that wide-range species had great effects on most of the zones and the recruitments of the shallow species may be very important in Zone 3W and 4.

An alternative method can use the results of SIMPER for analysis of species contributions. This approach was similar to the calculation of relative taxa contribution (Figure 8); however, in this case, the species contributions were categorized into co-existing ranges and the sum of the species contributions would be the contribution of that particular range to the average faunal similarity in the zone. The euryzonal and slope species had the highest contribution (50-70%) in the zones (Table 7). The importance of the euryzonal species tended to increase toward the deeper zone, while the importance of

slope species seemed slightly decreased. Using the same concept, the contributions of the co-existing ranges to the average faunal dissimilarities between the independent stations and their adjacent zones were calculated (Table 8). Between Zone 3W and 3E to GKF, the euryzonal and slope species had the highest contributions (43% and 36%, respectively). Contradictorily, the narrower species, such as the stenozonal species of Zone 1 and the species co-occurred in Zone 1 and 2E, explained highest faunal dissimilarity between Zone 1 and WC5 (27%). The euryzonal and slope species were still important, however, only explaining 23% of the faunal dissimilarity between Zone 1 and WC5. In general, the results of species range analyses agreed with the species contribution analysis, the broad-range species made large contributions to the similarity of faunal zones.

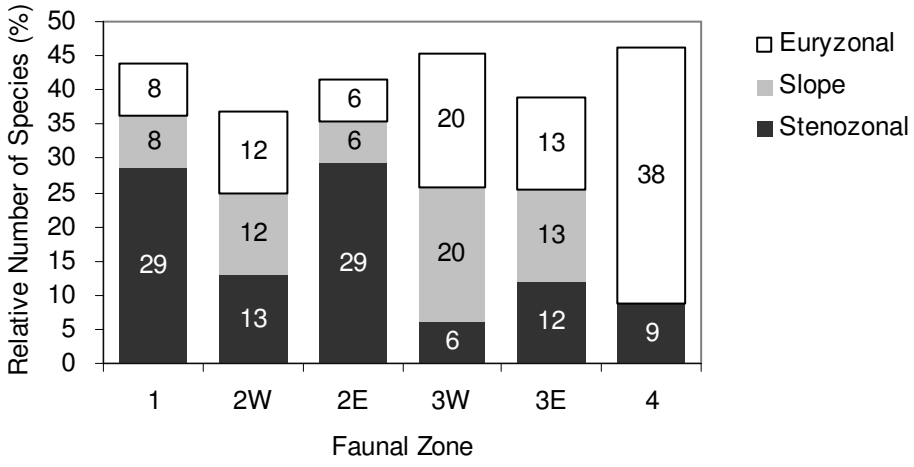

Fig. 9.Euryzonal, slope, and stenozonal species in each faunal zone.

Table 7. Contributions of species range to average Bray-Curtis similarity in faunal zones. The table only lists the ranges that contributing more 3% in at least one zone. * denotes the 5 most contributed species ranges.

Species Range	Zone 1	Zone 2W	Zone 2E	Zone 3W	Zone 3E	Zone 4
1,2W,2E,3W,3E,4	28.9*	48.3*	30.2*	55.2*	51.1*	64*
1,2W,2E,3W,3E	20.6*	18.6*	18.4*	14.8*	12*	0
1,2W,2E,3E	14*	4	11.6*	0	4.6*	0
1,2W,2E	5.7*	6.3*	8.8*	0	0	0
2W,2E,3W,3E	0	5*	3.6	6*	5.7*	0
2W,2E,3W,3E,4	0	2.7	0.6	7.7*	5	3
1,2W,2E,3E,4	2	0.6	2.4	0	2.9	8.7*
2E,3W,3E,4	0	0	0.1	8.5*	3.3	3.9*
1,3W,3E,4	0	0	0	0.2	2	11.6*
1,2E	7.9*	0	4.9*	0	0	0
1,2E,3E	5.5*	0	2.7	0	4.4*	0
2W,3W,3E,4	0	0.2	0	0.4	2.3	7.4*
2W,2E	0	4.4*	3.6	0	0	0
1,2W,2E,3W	2.3	3.6	1.7	0.2	0	0
1,2E,3E,4	3.6	0	1.5	0	0.3	0
1	3.6	0	0	0	0	0

Table 8. Contributions of species range to the average Bray-Curtis dissimilarity between zone 3W to GKF, zone 3E to GKF, and zone 1 to WC5. The table only lists the ranges that contributing more 3% in at least one zone. * denotes the 5 most contributed species ranges.

Species Range	3W/GKF	3E/GKF	1/WC5
1,2W,2E,3W,3E,4	24.6*	19.8*	12.5*
1,2W,2E,3W,3E	18.4*	16.1*	10.4*
1,2W,2E,3E	3.4*	8.4*	7.9
1,2E,3E	3.4	8.1*	5.5
1	1.6	1.3	13.8*
2W,2E,3W,3E	6.3*	7*	0
1,2E	0	0	13.2*
1,2W,2E	1.9	1.5	8*
2W,2E,3W,3E,4	4.3*	3.2	0.5
1,2E,3W,3E	2.9	2.6	1.9
2E	3.1	2.5	1.5
3E	0	5.3	0.5
WC5	0	0	5.7
2E,3W,3E,4	3.4	1.9	0
1,2E,3W	1.8	0	3.4
2E,3E	1.9	3.3	0

3.2. Standing stocks in faunal zones

The overall density decreased exponentially with depth (Figure 10, $Y= 6787.5\, e^{-0.74X}$, $R^2 = 0.74$, $P<0.001$). One way ANOVA supported significant difference of density among the faunal zones (Table 9). The multiple comparisons and the 95% confidence level (95CL) of the data suggested significant differences between most pairs of the faunal zones ($p<0.05$), except between Zones 1 and 2E, Zones 2W and 3E, and Zones 3W and 3E (Figure 11a). Four levels of animal densities were identified:

1) Zone 1 and 2E had the highest density (2594-11,233 individuals/m^2, 95CL). However, besides the head of the Mississippi Canyon (MT1) with 21,663 individuals/ m^2 (SE= 2499, n= 10), the second highest densities were only around 5000 to 6000 individuals/ m^2 at the shelf break sites (RW1, W1, C1, and S44), within the Mississippi (MT2 and MT3) and the Desoto Canyon (S35), and close to the mouth of the Mississippi River (Hipro). The two deepest sites in this category, Hipro and S36 (1572m and 1828m, respectively), had the mean densities about 3 times higher than other sites at similar depths (Figure 10).
2) Zone 2W and 3E had the second highest density (981-1985 individuals/m^2, 95CL).
3) Zone 3W and 3E had the third highest density (661-1777 individuals/m^2, 95CL). Site S5 of Zone 3E was sampled at the deepest part of the Mississippi Fan (3314m) and had a density about 3 to 5 times higher than other deep stations (S1-4).
4) Zone 4 had the lowest density (288-718 individuals/m^2).

In general, the animal density decreased across Zone 1 to Zone 4 and the high density seemed to occur in the vicinity of the Mississippi or De Soto Canyon in the northeastern GoM.

Table 9. Analysis of variance for mean standing stocks and α diversity in faunal zones (DF= degree of freedom, SS= sum of square, MS= mean square).

Variable	DF	SS	MS	F	P
Density	5	6.24	1.25	46.31	<0.001
Error	43	1.16	0.03		
Biomass	5	6.24	1.25	46.31	<0.001
Error	43	1.16	0.03		
E(S100)	5	4906	981	12.66	<0.001
Error	43	3332	77		
Evenness(1-λ')	5	0.02	0.005	2.11	0.08
Error	43	0.10	0.002		

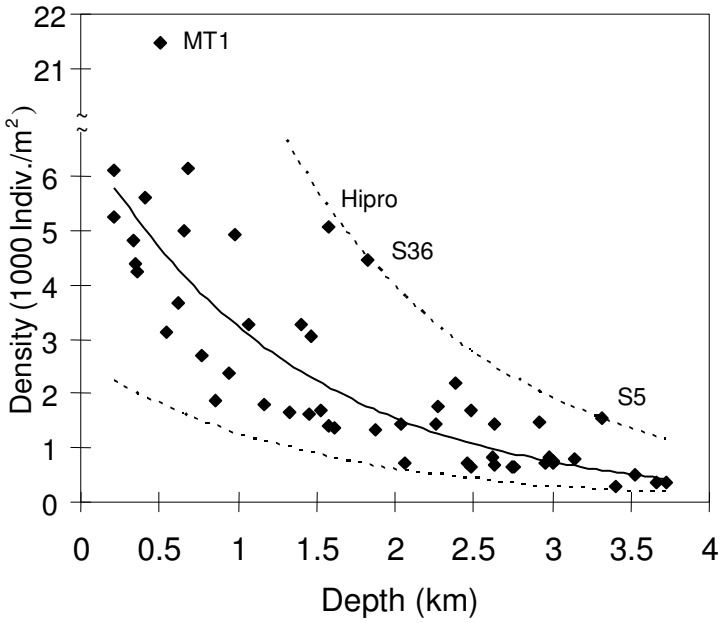

Fig. 10. Macrofauna density as a function of depth. The equation for relationship is Y= $6787.5\,e^{-0.74X}$ ($F_{1,49}$ =140.9, r^2 =0.74, P<0.001).

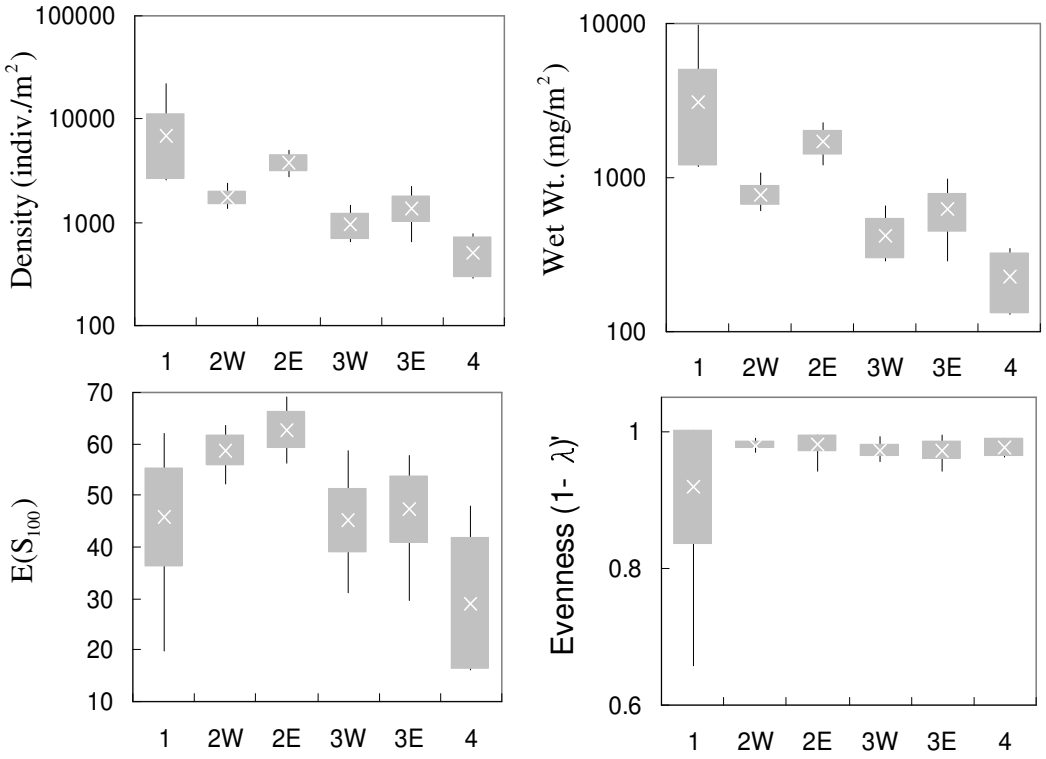

Fig. 11. (a) Mean density, (b) biomass, (c) expected number of species, and (d) species evenness in each faunal zone. The white cross indicates the mean values, gray box indicates 95% confidence level, and vertical line indicates the range between maximum and minimum value.

In order to examine the horizontal variation of animal abundance, regression analyses of mean density and depth were conducted on transects (RW, W, C, MT, S35-38, and S39-44, Figure 12). Most transects were best fit by exponential relationships with high coefficients of determination (R^2 = 0.84-0.99, $P<0.01$). There were three different rates of decrease in density with depth:

1) Transect MT and S35-38 had the highest faunal density as well as most rapid rates of decreasing stocks.

2) Transect RW, W, and S39-44 showed almost identical density trends with low faunal densities and slow decreases.
3) Transect C with moderate density and a rate that was comparable with transect RW, W, and S39-44.

The trend of decreasing faunal density converged at the base of the continental slope (~3000m), where the lowest faunal densities were observed. However, transect C somehow maintained slightly higher density than the other transects in deep water (2500-3000m). These patterns seemed to correspond to the geographic distances away from the mouth of the Mississippi River. Transect MT and S35-38 represented the "canyon" slope system with high stocks and rapid rates of decreasing density with depth. Transect RW, W, and S39-44 was generalized as the "normal" slope system with low densities and a slow decrease with depth. Transect C seemed to be a transition between "canyon" and "normal" slope systems. Thus, ANCOVA was performed to test the null hypothesis that the rates of decreasing density and mean densities were not different between the "normal" and "canyon" slope system. Prior to the test, data were logarithm transformed to approximate a normal distribution. The results suggested the rates of decreasing density were not significantly different ($F_{3,20}$ =1.3, P= 0.3) but the mean density was higher in the "canyon" than in the "normal" slope system ($F_{3,20}$ =5.17, P=0.008).

The macrofauna biomass was estimated from the wet weights and carbon weights of the 6 slope stations and 4 abyssal stations. The general trend also followed an exponential decrease with depth (Figure 13a, b). The mean body size was estimated

using the mean biomass divided by the mean density, which can be illustrated as regression models (Figure 13c, d). The slopes of the model illustrate the mean individual size. The intercepts were not considered in the estimation, since the biomass was zero when no animals exist. Thus, the mean macrofaunal size in the northern GoM was estimated to be 0.45 mg/individual and 0.02 mg-C/individual. The mean biomass was estimated from the mean density and mean macrofauna size (0.45 mg/individual). Therefore, the pattern of biomass (Figure 11b) was the same as density (Figure 11a). Four levels of macrofaunal wet weights (the 95CL) were estimated, including the highest biomass in Zone 1 and 2E (1.1 to 5.1 g/ m^2), the second highest biomass in Zone 2W and 3E (0.4 to 0.9 g/m^2), the third highest biomass in Zone 3W and 3E (0.3 to 0.8 g/ m^2), and the least biomass in Zone 4 (0.1 to 0.3 g/ m^2).

At the independent stations, the mean density and wet weights in GKF were 737 individuals/m^2 and 0.3 g/m^2. These values were at the upper bound of Zone 4 and the lower bond of Zone 3W, suggesting low standing stocks comparing to the adjacent faunal zone (Zone 3W and 3E). The mean density and wet weights in WC5 was 4382 individuals/m^2 and 2 g/m^2. Both were in the ranges of Zone 1 and Zone 2E.

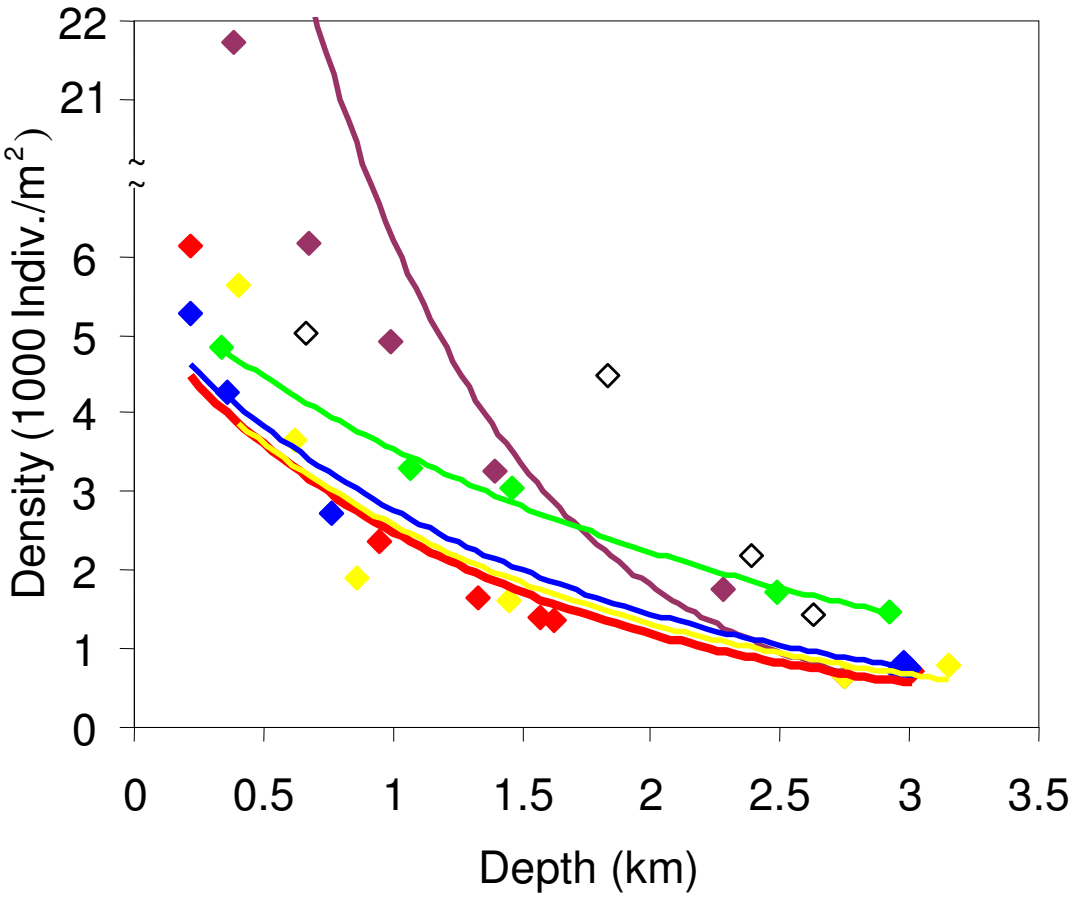

Fig. 12. Macrofauna density as a function of depth for transects. (1) Transect RW (red). $Y=5229.47e^{-0.74X}$, $r^2 = 0.88$, $F_{1,4} = 39.27$, $P= 0.003$. (2) Transect W (yellow). $Y=5068.86e^{-0.67X}$, $r^2 = 0.84$, $F_{1,4} = 26.45$, $P= 0.007$. (3) Transect S39-44 (blue). $Y=5319.94\ e^{-0.65X}$, $r^2 = 0.98$, $F_{1,4} = 284.96$, $P< 0.001$. (4) Transect C (green). $Y=5635.19\ e^{-0.46X}$, $r^2 = 0.99$, $F_{1,3} = 374.16$, $P< 0.001$. (5) Transect MT (purple). $Y=21743.87\ e^{-0.65X}$, $r^2 = 0.87$, $F_{1,4} = 35$, $P= 0.004$. (6) Transect S35-38 (black). $Y= -1782.83X+6630.62$, $r^2 = 0.72$, $F_{1,2} = 8.66$, $P= 0.1$.

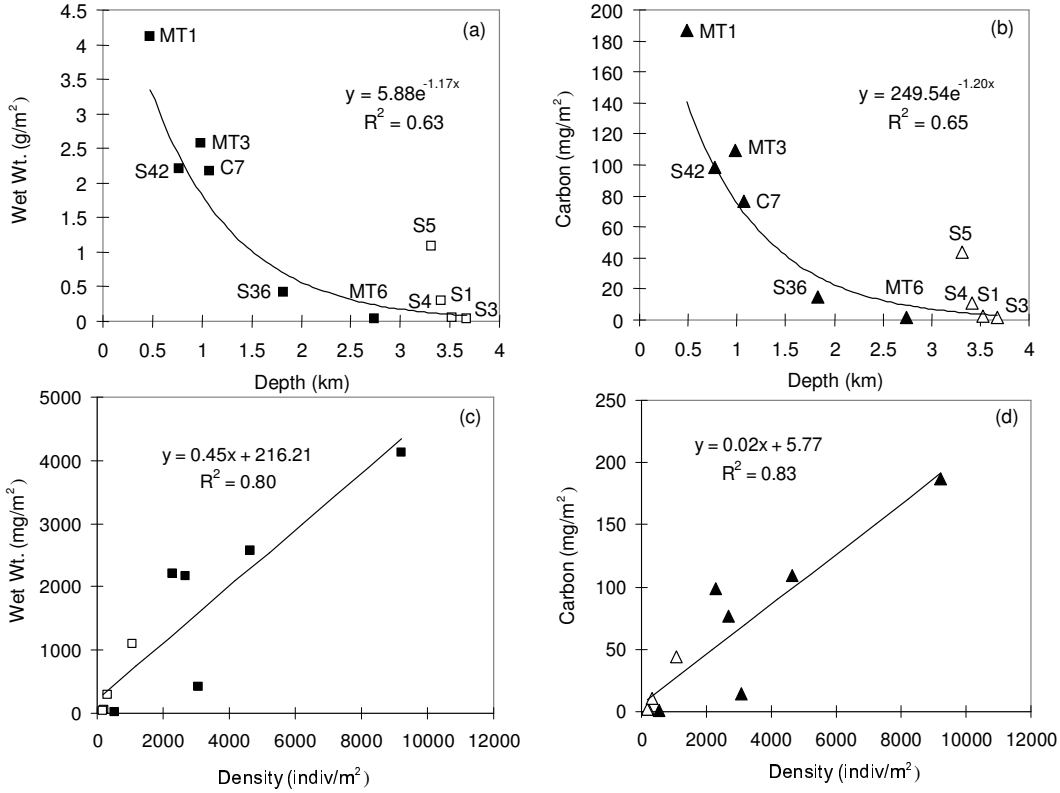

Fig. 13. Estimation of macrofauna biomass. Closed symbol represents sub-core samples from the slope and open symbol represents box-core samples from abyssal plain. (a) Mean wet weight as a function of depth ($F_{1,8}$ = 13.68, P<0.01); (b) Mean carbon weight as a function of depth ($F_{1,8}$ = 43.66, P<0.001); (c) Mean wet weight as functions of mean density ($F_{1,8}$ = 32.73, P<0.001); (d) Mean carbon weight as functions of mean density ($F_{1,8}$ = 38, P<0.001).

3.3. Biological diversity

3.3.1. α diversity

The same species abundance data for cluster analysis were used to examine the biological diversity. Due to the large variation of animal abundance, the sample size was

standardized to both 100 and 50 individuals in the richness measurement. For example, when $E(S_{100})$ is used, there were 10 stations (2465-3732m) having less than 100 individuals identified to species (Table 10); therefore, an underestimation of the species number could occur at the deepwater sites. In contrast, when $E(S_{50})$ is used, rarefaction may underestimate the species numbers at 80% of the sites, where there were about 100 to 10,000 individuals identified; hence, both $E(S_{100})$ and $E(S_{50})$ should be considered. Generally, the $E(S_n)$ reached a maximum at intermediate depths and declined toward shallow and abyssal depths (Figure 14), suggesting a quadratic relationship between $E(S_{100})$ ($F_{2,48}$=29.35, P<0.01) and $E(S_{50})$ ($F_{2,48}$=17.66, P<0.01) to depth. The models predicted the maximum diversity of $E(S_{100})$ = 57 and $E(S_{50})$ =35 at 1382 and 1515m, respectively. The unimodal trends of $E(S_{100})$ and $E(S_{50})$ were similar; except the curvature of $E(S_{50})$ was smaller and the predicted maximum diversity was deeper. One way ANOVA indicated significant main effects of $E(S_{100})$ on faunal zones. The multiple comparisons and 95CL of $E(S_{100})$ in each zone suggested 2 levels of expected number of species (Figure 11c), including the high $E(S_{100})$ in Zone 2W and 2E (55-66 species), and low $E(S_{100})$ in Zone 1, 3W, 3E, and 4 (16-55 species). Within the high $E(S_{100})$ areas, the highest values were found at C7, C4, S42, MT4 (64-69 species) in Zone 2E. On the other hand, the lowest $E(S_{100})$ were found at S1-5 (18-30 species) in Zone 4, as well as at MT1 (20 species) in Zone 1. The $E(S_{100})$ in the independent sites (GKF and WC5) were 32 and 39 species, respectively, implying the relatively low richness compared to their adjacent faunal zones. However, it was probably not true in GKF. Since only 60 specimens have been identified in GKF (Table 10), $E(S_{100})$ might potentially

underestimate the numbers of species. From a more appropriate measurement, $E(S_{50})$, the estimated numbers of species did not seem to particularly low compared to other sites at similar depths (Table 10).

Table 10. Standing stocks and diversity in DGoMB stations. Note: n = numbers of box core replicate, D = mean density (individual/m^2), SE = standard error, B = wet weight (g /m^2), N = numbers of identified specimen, S = numbers of species, $E(S_{100})$ = expected number of species for a sample of 100 individuals, $E(S_{50})$ = expected number of species for a sample of 50 individuals, 1-λ'= evenness index.

Zone	Station	n	D	SE	B	N	S	E(S50)	E(S100)	1-λ'
1	MT1	10	21663	2499	9.7	11262	163	13	20	0.66
	MT2	4	6172	414	2.8	1560	144	27	40	0.96
	RW1	5	6137	1436	2.8	603	170	38	62	0.98
	W1	5	5626	1491	2.5	513	95	25	40	0.83
	S44	5	5262	1045	2.4	349	102	35	55	0.97
	HiPro	5	5076	572	2.3	383	76	27	40	0.93
	C1	5	4829	1082	2.2	562	129	34	54	0.98
	S43	5	4265	983	1.9	282	93	32	51	0.98
	BH	5	3143	208	1.4	446	99	32	49	0.97
2W	RW2	5	2370	486	1.1	305	122	38	63	0.99
	W3	5	1883	376	0.8	320	118	35	58	0.97
	WC12	5	1787	383	0.8	204	93	39	64	0.99
	NB2	5	1700	423	0.8	213	92	36	59	0.98
	RW3	5	1641	405	0.7	174	79	36	57	0.98
	W4	5	1621	179	0.7	122	70	36	61	0.98
	RW4	5	1399	295	0.6	227	87	35	55	0.98
	RW5	5	1372	169	0.6	161	68	34	52	0.98
2E	S35	5	5019	628	2.3	762	183	37	62	0.98
	MT3	10	4924	660	2.2	1754	269	37	61	0.98
	S36	12	4481	522	2.0	1006	186	36	58	0.98
	W2	4	3662	271	1.6	535	150	34	56	0.94
	C7	10	3293	389	1.5	789	214	41	69	0.99
	MT4	5	3262	560	1.5	583	168	39	64	0.99
	C4	5	3045	522	1.4	525	165	40	66	0.99
	S42	9	2709	286	1.2	481	176	39	66	0.99

Table 10. Continued

Zone	Station	n	D	SE	B	N	S	E(S50)	E(S100)	1-λ'
3W	B1	5	1446	297	0.7	116	51	31	47	0.99
	NB4	5	1443	432	0.6	160	72	34	54	0.97
	NB3	5	1342	203	0.6	135	71	36	59	0.98
	B3	5	814	110	0.4	146	52	27	42	0.97
	RW6	5	715	150	0.3	112	43	28	41	0.96
	NB5	5	706	123	0.3	120	48	28	43	0.96
	B2	5	676	56	0.3	89	41	28	41	0.98
	W5	5	659	104	0.3	75	31	25	31	0.96
	AC1	5	637	154	0.3	96	49	33	49	0.99
3E	S37	5	2192	238	1.0	318	86	31	48	0.96
	MT5	5	1763	329	0.8	239	96	36	58	0.99
	C14	5	1709	114	0.8	385	90	31	48	0.98
	S5	2	1545	310	0.7	252	45	20	30	0.94
	C12	5	1485	246	0.7	245	84	32	51	0.97
	S38	5	1445	253	0.7	170	58	30	45	0.96
	S41	8	828	163	0.4	128	61	33	53	0.99
	W6	5	804	104	0.4	136	45	27	39	0.97
	MT6	9	638	105	0.3	154	70	34	54	1.00
4	S39	5	769	127	0.3	90	48	34	48	0.99
	S40	4	729	196	0.3	62	40	34	40	0.98
	S1	2	516	122	0.2	56	21	20	21	0.96
	S2	2	362	84	0.2	38	18	18	18	0.96
	S3	1	348	n/a	0.2	41	21	21	21	0.97
	S4	4	294	42	0.1	56	26	25	26	0.99
	WC5	5	4382	1089	2.0	725	114	24	39	0.76
	GKF	5	737	59	0.3	60	32	29	32	0.98

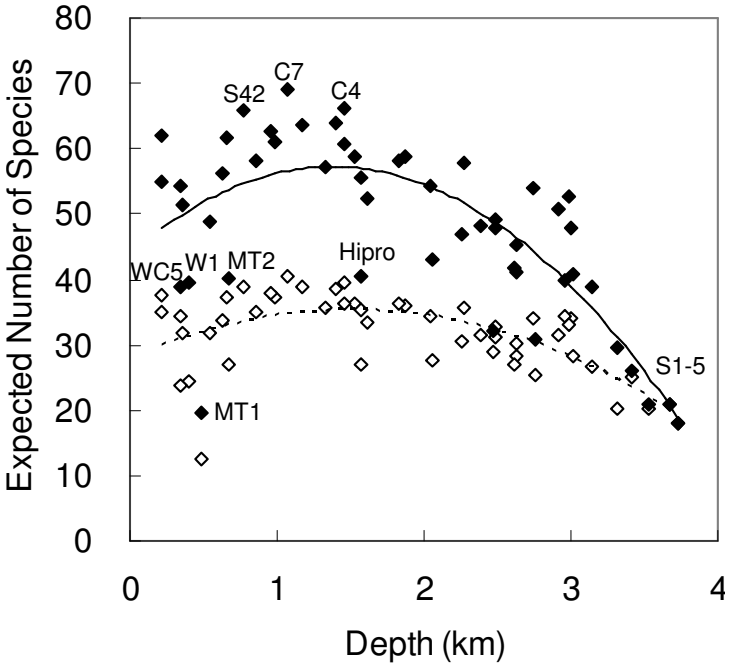

Fig. 14. Expected number of species as function of depth. The samples are randomly selected 100 (close rectangular) and 50 (open rectangular) individuals as functions of depth. The relationship for $E(S_{100})$ is $Y = 44 + 19X - 7X^2$ ($r^2 = 0.55$, $F_{2,48} = 29.4$, $P < 0.001$) and for $E(S_{50})$ is $Y = 28 + 10X - 3X^2$ ($r^2 = 0.40$, $F_{2,48} = 17.6$, $P < 0.001$).

In the equitability measurement, Zone 1 had the largest variation of species evenness (Figure 11d). However, MT1 and W1 were the only two sites with low species evenness (0.66 and 0.83, respectively). The evenness in the rest of the sites was between 0.93 and 0.98 (Table 10). In Zone 2W, 2E, 3W, 3E and 4, species evenness were high and steady between 0.94 and 0.99. In the independent stations, the species evenness was 0.98 in GKF and 0.76 in WC5. Therefore, beside MT1, W1, and WC5, the species evenness was generally high with small variation.

3.3.2. β diversity

The RELATE routine suggested the β diversity (Bray-Curtis dissimilarity) was significantly correlated to the Euclidean distances of sampling depths (Spearmen's rank, ρ=0.7, P<0.001). A two-way cross ANOSIM was used to test the null hypothesis that depths and east or west of the northern GoM had no effect on the β diversity. The factors included the "treatment" of the east or west of west longitude 91°and the "block effect" of the four different depth ranges (1km increment). ANOSIM suggested that there were both significant "treatment" (R=0.321, P<0.001) and "block" effects (R=0.62, P<0.001). The pairwise tests suggested all four depth ranges were significantly different from each other (P<0.05/6, Bonferroni correction) and a clear separation was observed among the depth ranges (R=0.4~0.9); therefore, by removing the "block effect", the species composition of macrobenthos in the northeastern GoM was significantly different from the northwestern GoM. In addition, according to the test statistic (R) of the ANOSIM, the "block effect" had better separation than the "treatment effect" (larger R), suggesting that depth was a more important factor controlling the β diversity.

In order to estimate the turnover of β diversity with depth, site RW1, W1, C1, and S44 (213-405m) were chosen as reference stations to compare their β diversities versus any given stations. The dissimilarities were excluded when the reference stations were compared with themselves. Regression analysis indicated a significant linear relationship between the mean dissimilarity and depth (r^2 = 0.74, P<0.001, Figure 15), in which the β diversity turnover (the slope of model) was 5.6 %/km, increasing from shelf break to

abyssal plain. This increase of dissimilarity with depth was relatively steady. At the shallowest sites (RW1 and S44), the mean dissimilarities to the reference sites were 65.9% and 69%, respectively. The deepest site (S2) had a mean dissimilarity of 91.8% to the reference sites. When the sampling area was divided into western and eastern parts by west longitude 91°, the faunal composition in the northeastern GoM appeared more similar to the shelf break fauna than in the northwestern GoM (Figure 15). However, ANCOVA does not support a significant difference in slopes ($F_{1,47}$ =0.7, P=0.41) or mean dissimilarities ($F_{1,47}$ =1.40, P=0.24) between eastern and western sites to the reference stations. That is, the rates of change in β diversity, as well as the species composition, were the same across the east and the west transects.

The characteristic β diversity of each zone can be calculated from the average within-zone dissimilarity. The highest β diversity was found in Zone 1, followed by Zone 3E, 4, 2E, 2W, and 3E with average faunal dissimilarity between 63.1 to 71.6% (Table 11). The hierarchical clustering, however, is a technique to explore the nature of the grouping; therefore, the faunal dissimilarities were minimized during the process of defining the homogeneous groups, contributing the small variation of β diversity among the faunal zones.

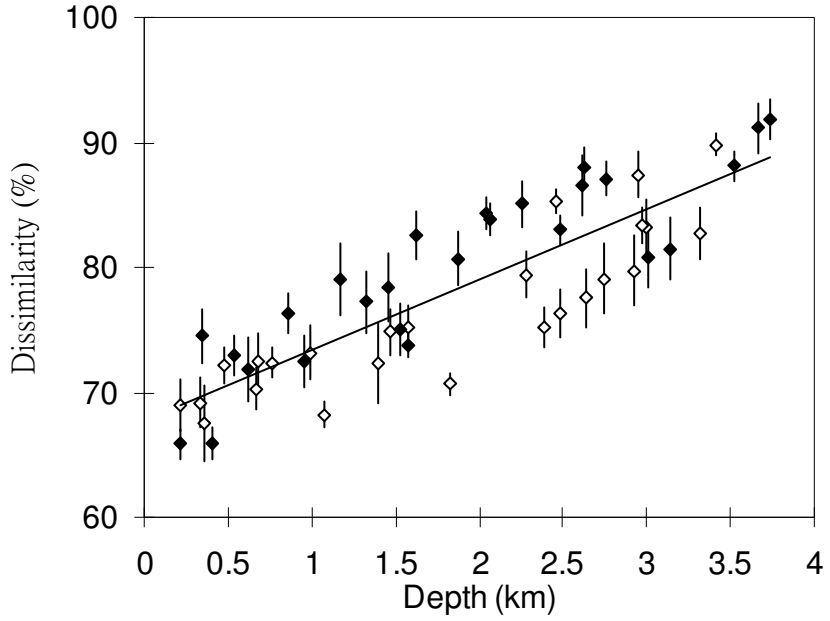

Fig. 15. Mean Bray-Curtis dissimilarity between reference sites (RW1, W1, C1, and S44) and any given station as a function of depth. The equation for the relationship is Y = -5.6X+ 32.2 ($F_{1,49}$ =140.6, r^2 =0.74, P<0.001). Error bars represent ± 1 standard error. Open diamond represents east of west longitude 91˚west and closed diamond represents west of west longitude 91˚W..

Table 11. Standing stocks and diversity (α, β, γ) in faunal zone with ± 1 standard errors. Note: n = number of stations, D = mean density (individuals/m^2), B = wet weight (mg/m^2), $E(S_{100})$ = expected number of species from random selected 100 individuals, 1-λ'= evenness index, Dissim. = mean Bray-Curtis dissimilarity, Sobs = observed species richness.

		Standing stocks		α		β	γ			
Zone	n	D	B	$E(S_{100})$	1-λ'	BC	Sobs	Chao2	ICE	Jack2
1	9	6908±1871	3109±842	46±4	0.92±0.04	71.6	512	919	967	911
2W	8	1721±111	775±50	59±1	0.98±0.00	63.1	326	515	580	547
2E	8	3799±314	1710±142	63±2	0.98±0.01	64.1	640	942	1012	1024
3W	9	937±120	422±54	45±3	0.97±0.00	63.1	199	381	394	357
3E	9	1379±173	620±78	47±3	0.97±0.01	68.1	291	513	533	509
4	6	503±84	226±38	29±5	0.98±0.01	67.9	104	332	318	209
Total	51	2653±450	1194±203	48±2	0.96±0.01	76.7	957	1361	1360	1498

3.3.3. γ diversity

From a total of 957 species based the 6 major macrofauna groups, the richness estimators (Chao2, ICE and Jacknife 2) predicted 1361 to 1498 species in the sampling area (Table 11); however, neither the observed nor estimated species accumulation curves reached the asymptote (Figure 16), indicating an underestimation of species richness. Among the faunal zones, Zone 2E had the highest γ diversities, followed by Zone 1, 2W, 3E, 3W, and 4 (Table 11); however, the estimations were similar between Zone 2W and 3E. The different estimators made close predictions in all zones except Zone 4. Chao 2 and ICE performed better than Jacknife 2 at relatively smaller sample size. However, none of these species accumulation curves approached the asymptote. In Zone 2W and 2E, species accumulation curves for Chao 2 and ICE seem close to the asymptotes while the last few samples were added in the inventories (Figure 17b, c), suggesting that these predictions might be close to the actual species richness. In Zone 1, 3W, 3E, and 4, the species accumulation curves still tended to increase at the end of the species inventories (Figure 17a, d, e, f), indicating that the species richness was greatly underestimated.

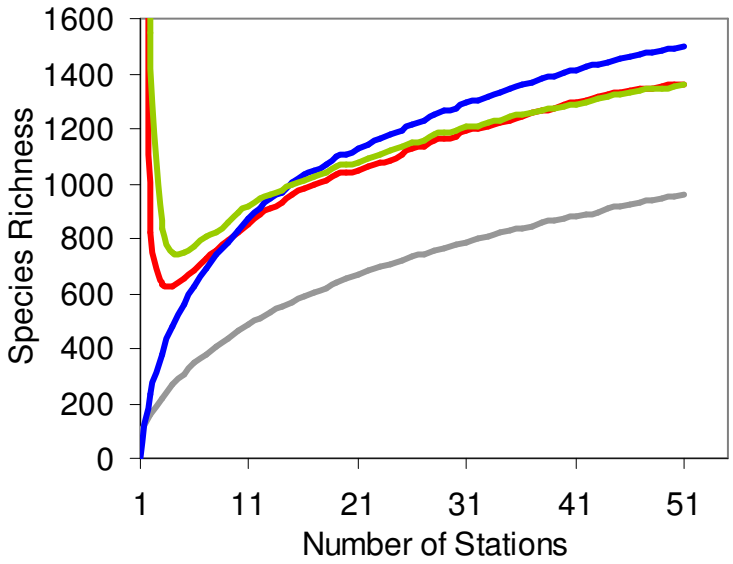

Fig. 16. Estimation of species richness in the northern GoM using species accumulation curves and incidence-based richness estimator. Note: Observed species richness (gray line), Chao2 (red line), ICE (green line), and Jacknife 2 (blue line).

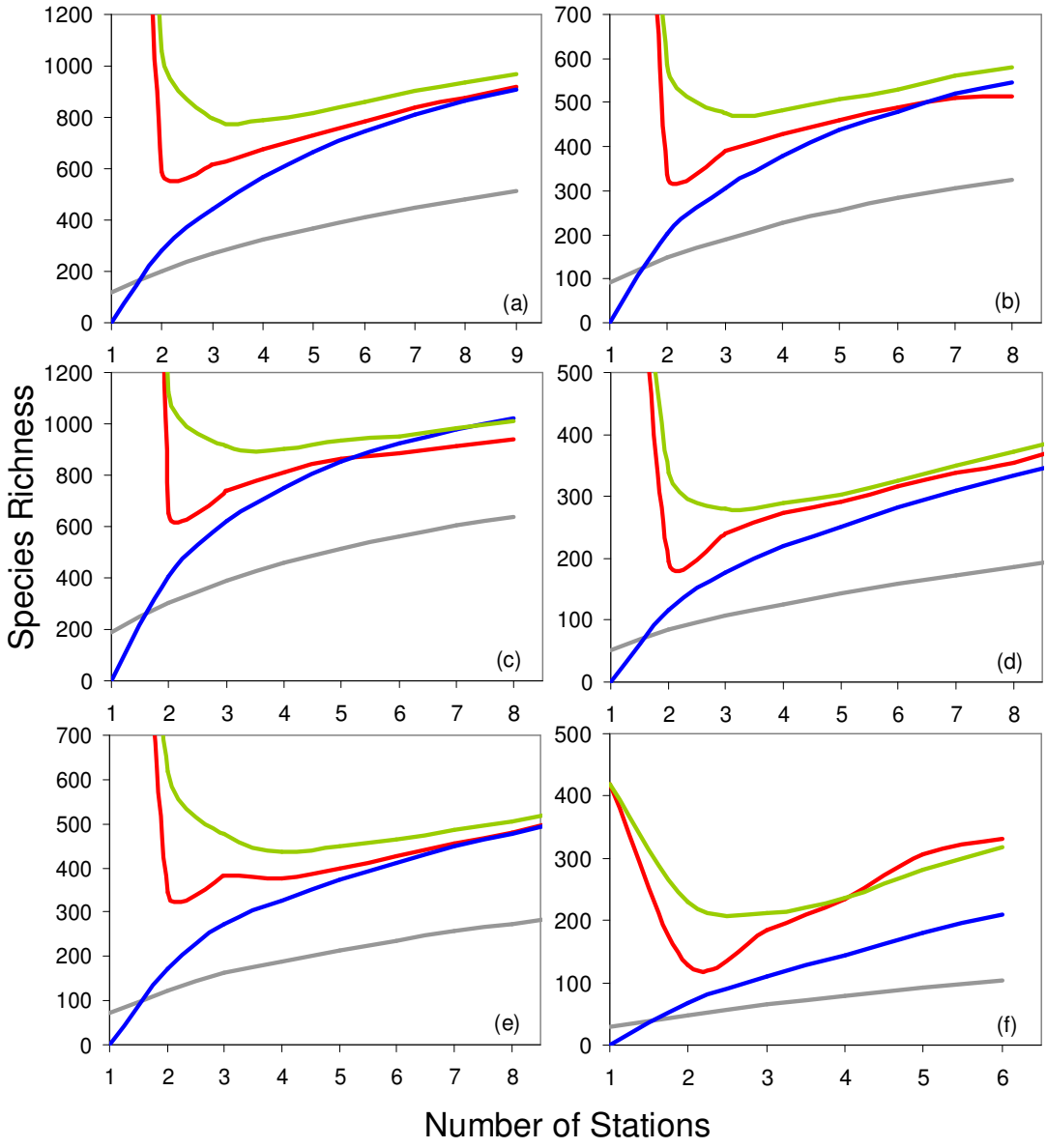

Fig. 17. Estimation of species richness in each faunal zone using species accumulation curves and incidence-based richness estimator. Note: Observed species richness (gray line), Chao2 (red line), ICE (green line), and Jacknife 2 (blue line). (a) Zone 1; (b) Zone 2W; (c) Zone 2E; (d) Zone 3W; (e) Zone 3E; (f) Zone 4.

3.4. Cumulative species renewal with depth

The cumulative species renewal is represented by summing the cumulative species appearance and disappearance in 100m depth increments. The slope of the curve indicates the rate of species renewal with depth. Theoretically, the species recruited with depth would eventually drop out of the assemblage, and so the cumulative appearance of species at the deepest site would almost be equal to disappearance of species. The last recruitment however would stay in the assemblage, and thus the cumulative species renewal ended up close to twice the observed species richness. The largest changes in the rate of species renewal occurred at 1200-1700m and 3000-3200m (Figure 17). The rapidest species renewal was from shelf break to 1200m, where 84% of total species appeared and 39% of total species disappeared. The species renewal nearly stopped at 1200-1400m, resumed again at 1400-1700m, and then continued changing at a steady rate until the deepest depth was reached. Nonetheless, there was a pulse due to the loss of species at 3000-3200m, where only 6 species were added but 104 species were dropped out of the assemblage. As a result, there are about two rates of species renewal with depth can be identified: 1) the rapid species addition from shelf break to 1200m, 3) the mild species renewal from 1400m to 3750m.

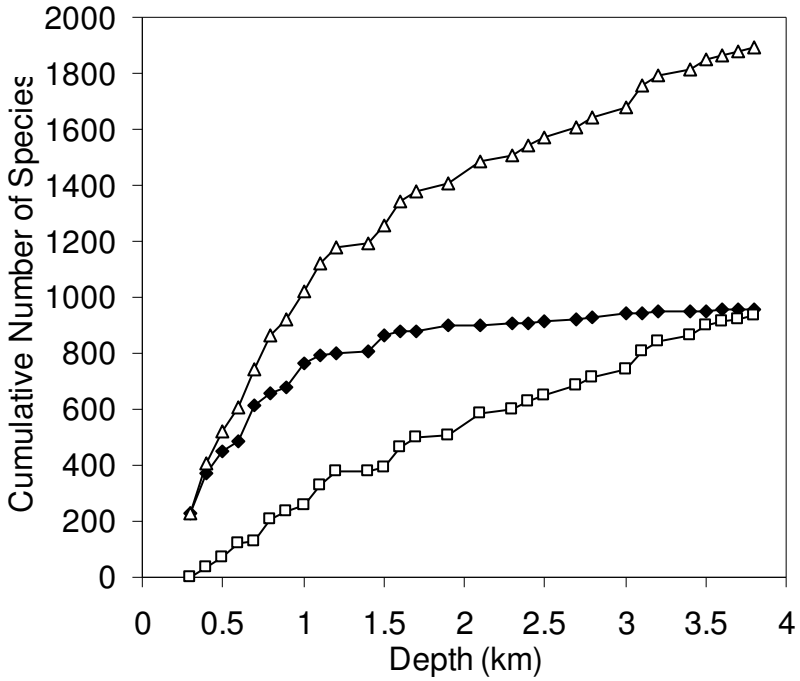

Fig. 18. Cumulative number of species renewal (open triangle), appearance (close rectangular), and disappearance (open square) with depth.

3.5. Linking environmental variable to community structure

The RELATE routine indicated a significant correlation between the Bray-Curtis similarities of species abundance and the Euclidean distances of 13 selected environmental variables (Spearman's rank, $\rho = 0.522$, $P=0.001$). The best subsets of environmental variables derived from BIOENV routine were the combinations of export POC fluxes, temperature, and trace metals (Table 12). The RELATE routine was conducted on each of the 13 variables, suggesting that the export POC fluxes had the highest correlation with the species abundance followed by other 12 variables listed in

table 13. One way ANOSIM of environmental variables indicated a significant main effect on faunal zones (R= 0.293, P<0.001). Pairwise tests suggested significant differences of environmental properties between every pair of faunal zones (P<0.05/15, Bonferroni correction), except between Zone 1 and 2E (P=0.031), between Zone 3W to 2W (P=0.006) and 2E (P= 0.011), and between Zone 3E and 4 (P= 0.037). Based on the RELATE routine (Table 13), the values of export POC fluxes, Sr concentration in the sediment, and bottom water temperature, were superimpose on MDS plot of species abundance to examine the animal-environmental relationship (Figures 19-21). The export POC fluxes showed a distinct zonal pattern with clear between-zone and small within-zone variation (Figure 19). Although the sampling depth, which was not included in these BIOENV or RELATE analyses, was actually given the higher correlation (ρ=0.7, p<0.001) to the species composition and distribution; there is no indication of depth variation between the east zones vs. west zones (Figure 5). The higher export POC fluxes to Zone 2E than to 2W, as well as to Zone 3E than to 3W (Figure 19) suggested the differences of food availability may be a more important factor than depth to explain the horizontal zonation. All four trace metals selected for analysis showed high correlation with species abundance (Table 13). The Sr concentration, as an example of the metals, illustrated the clear, high value in the Zone 4 and stable, low value in zone 1, 2W, 2E, 3W, and 3E (Figure 20). However, the distinct high value in S5 of Zone 3E suggested that the Sr concentration does not have significant effect on the faunal composition. The high correlations of metals to the faunal distribution are more likely due the auto-correlation with depth. The bottom water temperature was clearly higher in

Zone 1 than in other faunal zones (Figure 21), showing that its effect on faunal zonation may be only restricted to the shallow water.

Table 12. The best subsets of environmental data with the highest correlations to zonal pattern. Note: J (z) represents export POC fluxes.

No. Vars	Rho	Variable
1	0.698	J(z)
2	0.689	J(z), Pb
2	0.685	J(z), Ca
3	0.679	TEMP, J(z), Pb
3	0.67	J(z), Ca, Pb
4	0.669	TEMP, J(z), Ca, Pb
2	0.669	J(z), Sr
5	0.667	TEMP, J(z), Ca, Mn, Pb
4	0.665	TEMP, J(z), Mn, Pb
2	0.663	J(z), Mn
3	0.661	J(z), Pb, Sr
3	0.661	J(z), Ca, Sr
4	0.657	TEMP, J(z), Pb, Sr

Table 13. Correlation between single environmental variable and zonation pattern. Note: J (z) represents export POC fluxes.

Variable	Rho	P
J(z)	0.698	0.001
Sr	0.416	0.001
TEMP	0.387	0.001
POC	0.373	0.001
Pb	0.367	0.001
Mn	0.355	0.001
Ca	0.331	0.001
DO	0.283	0.001
% Sand	0.197	0.001
DOC	0.175	0.001
PAH	0.152	0.01
% Silt	0.139	0.014
Org-N%	0.102	0.049

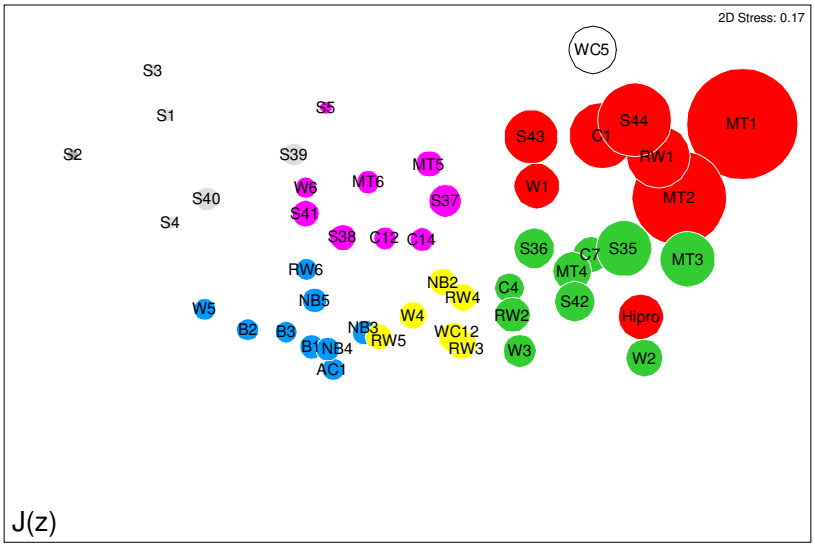

Fig. 19. Non-metric MDS plot superimposing export POC fluxes. The analysis is based on 4th root transformed data and Bray-Curtis similarity. Bubble size equals relative export POC fluxes and color schemes represent different faunal zones.

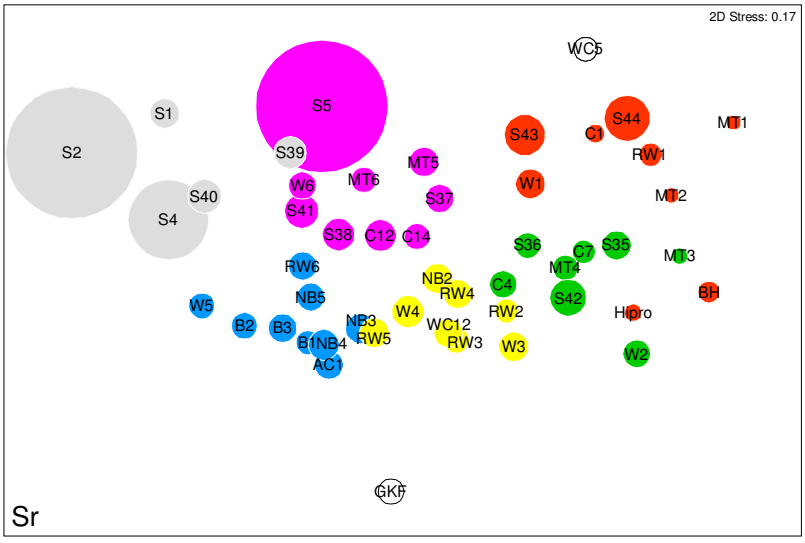

Fig. 20. Non-metric MDS plot superimposing Sr concentration. The analysis is based on 4th root transformed data and Bray-Curtis similarity. Bubble size equals relative Sr concentration and color schemes represent different faunal zones.

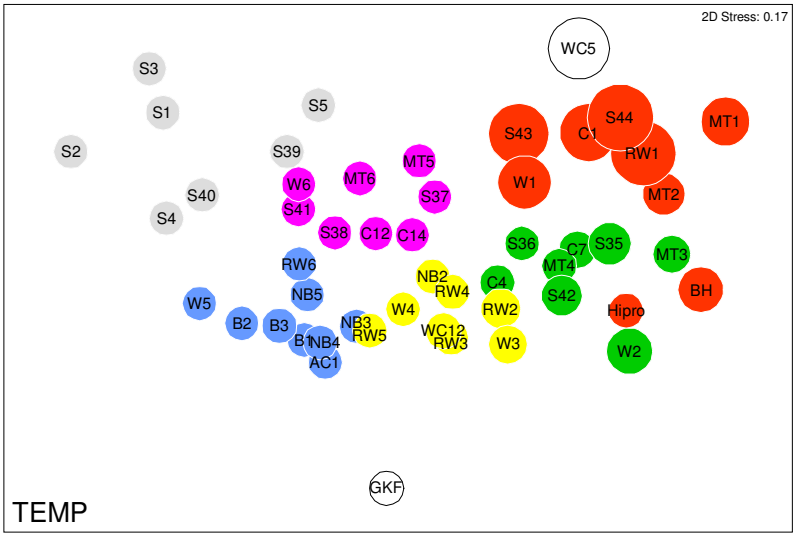

Fig. 21. Non-metric MDS plot superimposing temperature. The analysis is based on 4th root transformed data and Bray-Curtis similarity. Bubble size equals relative water temperature and color schemes represent different faunal zones.

3.6. Summaries of hypothesis testing

Based on the results, I accepted:

1) Significant faunal zones with distinct standing stocks, α diversities, and environmental properties exist.
2) Macrofauna density was significantly higher within submarine canyons than on the adjacent continental slope.
3) Both depth and longitude (E vs. W) had significant effects on β diversity.

There was no evidence that:

1) Rate of decrease in macrofauna density with depth was greater within the submarine canyons than on the adjacent continental slope.

2) Species (β diversity) turnover rate with depth was different from the northeastern GoM than the northwestern GoM.
3) The faunal composition was more similar to the shallow-water fauna in the northeastern GoM than in the northwestern GoM.

4. DISCUSSION

4.1. Bathymetric zonation

The pattern of faunal zonation in the deep sea varies among different regions and taxonomic groups (Gage and Tyler, 1991). The sharp rate of faunal replacement and discontinuity has been reported for megafauna (Menzies et al., 1973; Haedrick et al., 1975, 1980; Gage, 1986; Hecker, 1990; Howell et al., 2002). Macrofauna has been suggested to have a more gradual species replacement with depth in bathyal and abyssal zone compared to megafauna (Sanders and Hessler, 1969; Rowe et al., 1982; Olabaria, 2005). The difference in the size groups has been attributed to the dispersal capability of the macrofauna larvae during early life history (Gage and Tyler, 1991). In this study, species replacement was gradual without distinct faunal breaks or discontinuities. The species composition of the faunal zones was different, but at the same time, closely related, which agrees with previous work.

This study supports the exponential decline of macrofauna biomass with depth (Rowe, 1983). One interesting observation of this study was the distinct difference in standing stocks between east and west faunal zones (Figure 11a, b) at similar depth ranges. This horizontal faunal change provided an opportunity to tease out the cause of zonation without the “depth” effect. It is well established that seasonal enhancement of POC flux could increase benthic biomass (Rowe, 1983, 1998); therefore, the distinct standing stocks may suggest that the available food for benthic reproduction and

secondary growth was also different between the eastern and the western zones. The estimation of export POC fluxes has further confirmed these east-west variations of the benthic energy (Figure 19). Hence, based on each faunal zone having a distinct level of biomass, we proposed that the gradual, continuous, species replacement, or faunal zonation, takes palce on the declining gradient of food influx from the shallower zones to the deeper zones, as well as from the eastern zones to the western zones. That required level of energy may have determined the lower bound of the faunal zones, while the upper bound was more likely controlled via competition, predation, or changes in habitat geochemistry (Carney, 2005).

The submersion of faunal zones in the eastern upper-slope (Hipro) and the central GoM (S5), as well as the separation of east-west faunal zones (Figure 6), indicated that the terrestrial input of the Mississippi River has tremendous influence on the species composition and spatial variation of the benthic infauna. According to the sediment dispersal paths proposed by Balsam and Beeson (2003), the organic materials (clay) from the Mississippi River are transported westward along the shelf and southward onto the deep portion of Mississippi Fan (Figure 22). Deposit/suspension feeders can potentially benefit from the organic-rich sediments being pushed further offshore, and therefore, may be capable of thriving at deeper depths. On the other hand, the down-slope mass sediment movements and deep currents that drive the sediment dispersal, can carry planktonic larvae to deepwater, and cause the submergence of faunal zone in the central GoM. The close faunal composition between S5 and W6 (Figure 7e) may support this assumption, implying that the deep currents along the Sigsbee Escarpment is the

path of gene flow from the west side to east side of the lower slope (Figure 22).

Near the mouth of the Mississippi River, there was evidence of the river influence on the benthic biota. Biggs et al. (2006) suggested a seasonal variation of chlorophyll concentration associated with mesoscale eddies in the northeastern GoM during the summer months. These eddies transported the low salinity, high chlorophyll Mississippi River plume water off the shelf into the deep eastern GoM and contributed to a 2 to 3 fold increase of the chlorophyll concentration over the yearly average at Hipro. Despite the mid-slope depth (1572m), the community structure at Hipro has shifted to high abundance and low richness with species composition more closely resembling the upper slope fauna. Oddly, it is about this depth that the highest α diversities occurred in the northern GoM (Figure 13). Since the seasonal pulses of surface production could be transferred rapidly (>100m/day) to the deep-sea floor by sinking particles (Asper et al., 1992), the benthic community at Hipro might also experience the seasonal or annual variation of POC flux. Due to the high species evenness (1-λ'=0.93), the benthic community at Hipro was not dominated by a particular species. The physical instability caused by seasonal or annual energy variation seems to be the main cause of the shift of faunal composition and submergence of Zone 1 at Hipro in the eastern upper slope.

The Mississippi Canyon and Fan are the largest geological features in the northern GoM, as well as active conduits for transporting sediments and organic materials from the continental shelf to the deep-sea basin (Gardner, 1989). Mass wasting events, such as rock falls, mud slides, and turbidity flows have been reported in submarine canyons (Shepard et al., 1974; Coleman and Prior, 1988; Gardner, 1989). River flushing, storm

surges, earthquakes, strong currents, or the gravity of sediments and steepness of the canyon wall can trigger catastrophic events (Inman et al., 1976; Okey, 1997; Puig et al., 2004). Some investigators conclude that the physical disturbances, such as strong bed flows or the seasonal storm-induced sediment flushing are responsible for low diversity and high dominance of macrobenthos (Gage et al., 1995; Okey, 1997). On the other hand, in situ experiments suggest temporal, small-scale patches of organic enrichment and disturbance are important factors shaping the deep-sea communities (Grassle and Morse-Porteous, 1987; Snelgrove et al., 1996). Vetter and Dayton (1998) pointed out increasing stocks of infaunal invertebrate within Scripps/ La Jolla Canyon result from organic enrichment from the accumulation of macrophytes. In this study, we suggested that the exceptionally low diversity, high dominance, and high standing stocks of benthic infauna at the head of the Mississippi Canyon, with a distinct species composition from the canyon head (MT1) down to about 700m (MT2), are possibly related to the accumulation of organic materials from the Mississippi River and adjacent continental shelf. Macrophyte debris was also found in the trawl sample, including the water hyacinth, Sargassum, and wood pieces, presumably, from the coastal estuaries. However, unlike the Scripps/La Jola Canyon, the bottom of MT1 was not covered by dense macrophytes. The most distinct feature in the bottom photographs was the numerous patches of amphipod tubes. It might simply be that the kelp forest on the shelf of Scripps/La Jolla is a greater source of particulate organic matter. Alternatively, the small body size and large number (~16,000 individuals/m^2) of amphipod in MT1 may suggest that the accumulated organic matter is comsumed at high efficiency due to their

opportunistic characteristics. Snelgrove (1996) concluded that the different type, intensity, and aging of enrichment patches might affect deep-sea diversity by providing microhabitats, in which the opportunistic species can take advantage of the favorable resources during the early stage of succession. However, it is uncertain whether the organic enrichment or the physical disturbance was more important in shaping the community structure of the head of Mississippi Canyon. From the high species richness in MT1 (163 species, rank 9^{th} out of our 51 stations), the catastrophic events do not seem to cause chronic extinction. We assumed the dominance is related to competitive exclusion for organic materials, but rare species still co-exist with the dominant species.

In the cluster analysis, due to the low faunal similarities to other sites, WC5 and GKF, were not included in our defined faunal zones. Nonetheless, these independent sites may contain important information to understand the process of faunal change and the linkage between the environment and the faunal composition. Polychaete *Prionospio cristata* had the highest contribution to the faunal dissimilarity between WC5 and the adjacent upper-slope (Zone1). The high dominance (48.3% of total abundance) of *P. cristata* only occurs in WC5. Prionospio species are suspension/deposit feeder and usually inhabit soft muddy sediments; therefore, high silt (>33.9%) and clay (>47.1%) sediment were found in the sites with *P. cristata*. In fact, the sediments of WC5 had one of the highest silt contents (44.5%) among all sites. Although they also seem to prefer the clay sediments, there are fewer specimens in the sites with higher clay sediment (59.1%~65%) than WC5 (49.9%); hence, we suggest that the high dominance of P. cristata in WC5 is associated with the high silt content sediment. Several sites, including

MT4, Hipro, and GKF, with similar silt (44.5%~45.5%) and clay (45.5%~52.9%) percentage did not have any *P. cristata*, probably due the deeper depths in these stations (1401m~2465m). *Prionospio cristata* appeared to be a shallow-water species, with records at 6 sites shallower than 767m and only one site at 2042m. From the historical data (Callaway et al., 1988), *P. cristata* did not occur in WC5 during NGoMCS study. There were three Prionospio species contributing only 0.9% of the total abundance in WC5. The most dominant species was *Litocorsa antennata*, accounted for 18.2% of the total abundance. In contrast,, we did not find *L. antennata* in WC5 in the present study. There is also a dramatic difference in terms of the sediment grain size between two studies at WC5, where the silt content was only 18.6 % in NGoMCS. However, it would be too subjective to conclude that this temporal change was caused by the difference of sediment grain size. It may also reflect the seasonal variation, the changes of the benthic habitat, or a single settlement event. A revisit of WC5 and long term monitoring would be essential to further understand this temporal variation.

GKF is located between the east (Zone 3E) and west lower-slope (Zone 3W) and had a distinct faunal composition. This distinctiveness was mostly due to the compositional differences of euryzonal and slope species between GKF and the adjacent faunal zones (Table 8). GKF stands for the Green Knoll Furrows, which were recently discovered on the sea floor at the base of Green Knoll (Bryant et al, 2000). These mega-furrows, with size from 1 to 10 m deep and 5 to 50 m wide, are believed to be associated with strong near bottom currents, which Hamilton and Lugo-Fernandes (2001) proposed in the deep central GoM. The faunal composition of GKF is more close to the west

lower-slope (Zone 3W) and the west mid-slope (Zone 3E) than to their east counterparts (Zone 2W and 2E), implying a potentially western origin of fauna (Figure 5). It is still unclear that the faunal composition was associated with the direction of the bottom currents. We believe that GKF have selected a specific benthic assemblage adapted to this distinct geological feature with high current energy environment.

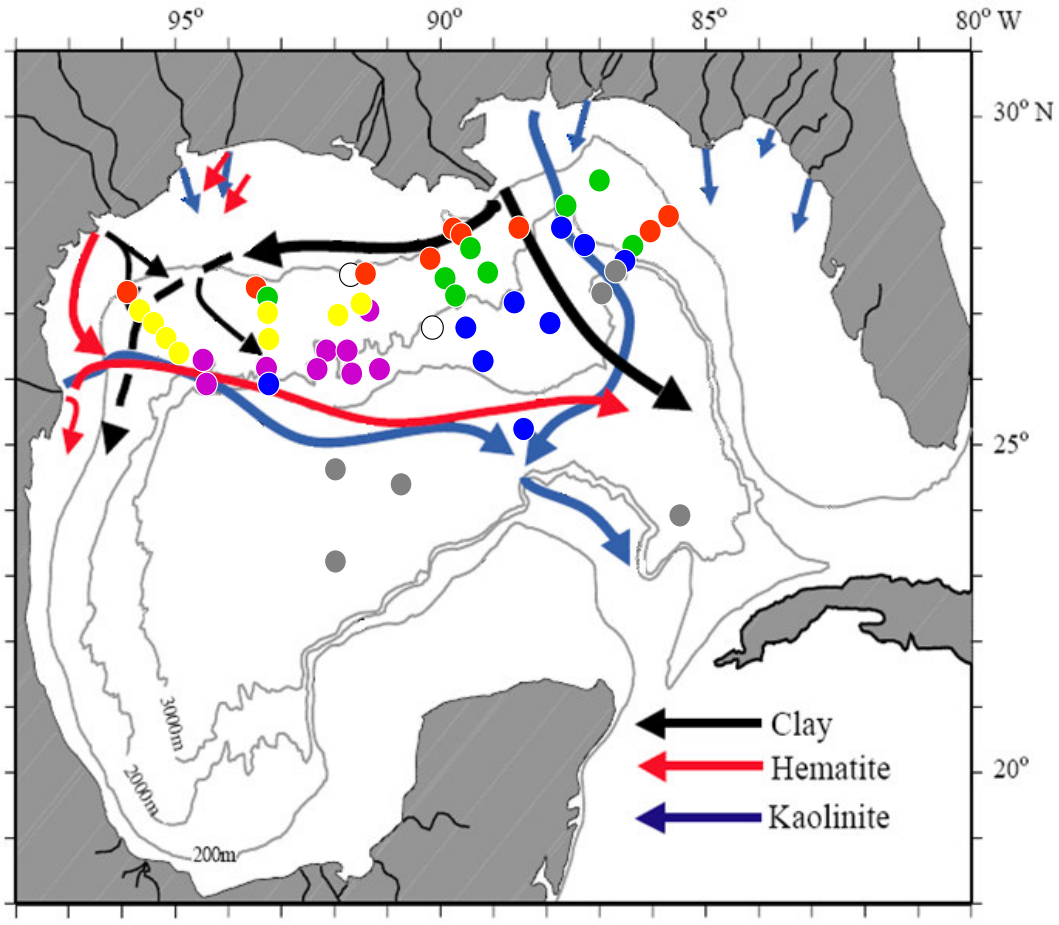

Fig. 22. Sediment dispersal paths on DGoMB stations. The color scheme represents faunal zones. Figure was modified from Balsam and Beeson (2003).

4.2. Standing stocks

When comparing the standing stocks to other ocean margins, the density of the northern GoM was comparable to North Atlantic (Figure 23), while the biomass was more close to the eastern Mediterranean (Figure 24). Rowe et al. (1974) concluded that both animal abundance and biomass were greater in the Atlantic than in the GoM. Nevertheless, we found that the animal biomass was lower in the Gulf than on most major ocean margins, such as the Atlantic and Pacific, but the level of animal density was comparable to, or even higher, implying the smaller body size in the GoM relative to other areas (Peguegnat et al., 1990). Some artifacts may lead to this disparity. Part of the DGoMB study has focused on investigating the benthic organisms in submarine canyons. The overall density might be elevated by these productive areas. However, when the canyon data were excluded, the regression model (Density= 5159*exp (-0.67*Depth), R^2 =0.83, $F^{1,38}$ = 187.77, P<0.001) was still similar to the North Atlantic (Figure 23). In addition, since the 420μm sieve was mostly used in the Atlantic studies, while 300μm was used in the DGoMB study, the high abundance in this study could be a result of the smaller screen size. However, it can only be validated by using the 300μm sieve in the future studies. In general, the rates of exponentially declining abundance with depth were very close among the four selected ocean margins (Figure 23), suggesting similar input of particulate organic materials at depths among different margins. On the other hand, the declining biomass was faster than the decreasing densities, indicating a decrease macrofauna size with depth (Figure 24).

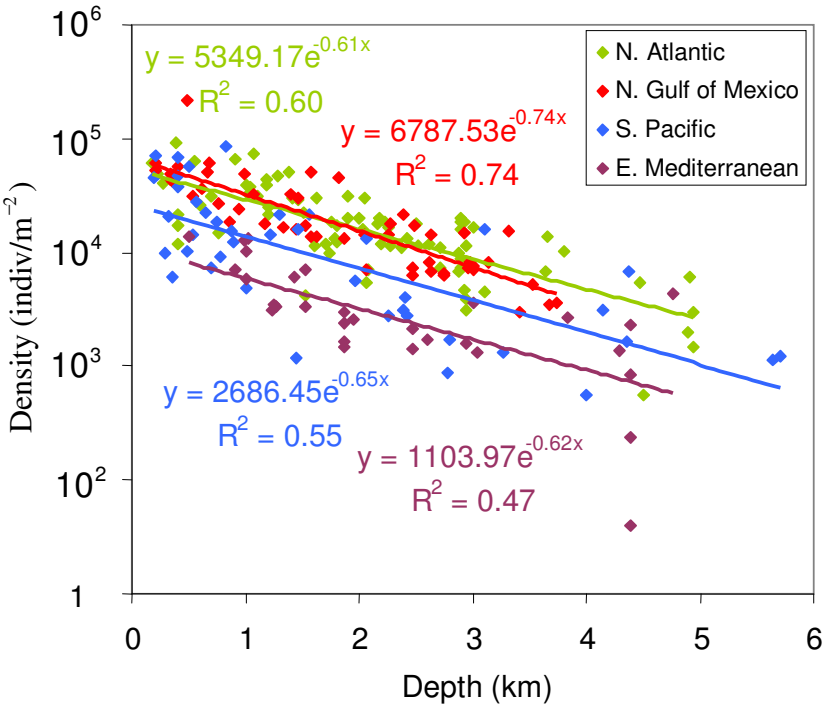

Figure 23: Macrofaunal density as a function of depth in the N. Atlantic (Sanders et al., 1965, 0.42mm; Rowe et al., 1982, 0.42mm; Galéron et al., 2000, 0.5mm; Gage et al., 2000, 0.42mm; Flach et al., 2002, 0.5mm), northern GoM (DGoMB, 0.3mm), eastern Mediterranean (Kröncke et al., 2003, 0.5mm), and S. Pacific (Rowe, 1971, 0.42mm; Hessler and Jumars, 1974, 0.3mm; ; Hyland et al., 1991, 0.3mm; Alongi, 1992, 0.5mm; Borowski and Thiel, 1998, 0.5mm; Borowski, 2001, 0.5mm; Smith et al., 2002, 0.3mm; Palma et al., 2005, 0.5mm). Note: reference is followed by the sieve size.

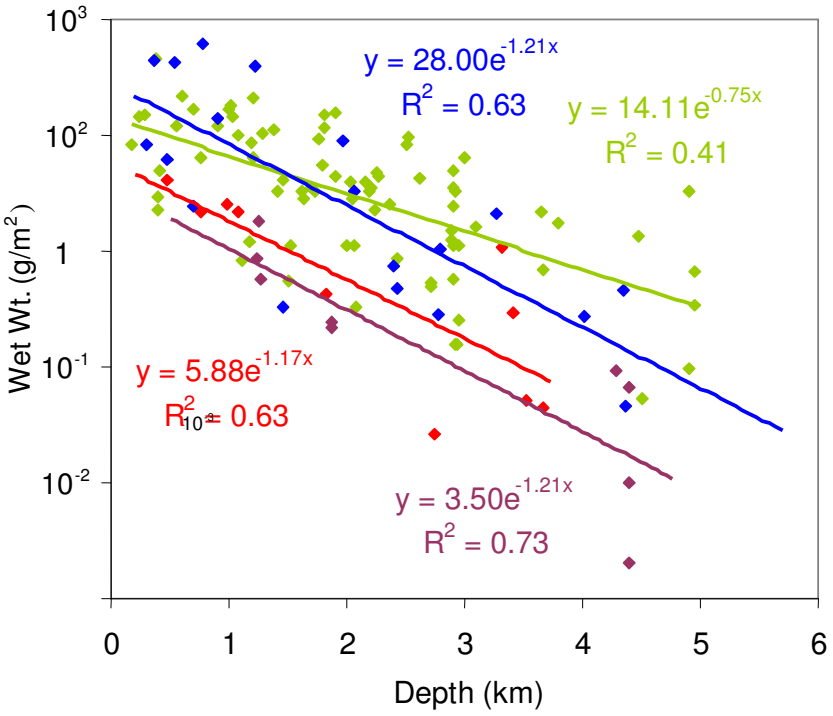

Figure 24: Macrofaunal wet weight as a function of depth in the N. Atlantic (Sanders et al., 1965, 0.42mm; Rowe et al., 1982, 0.42mm; Galéron et al., 2000, 0.5mm; Gage et al., 2000, 0.42mm; Flach et al., 2002, 0.5mm), northern GoM (DGoMB, 0.3mm), eastern Mediterranean (Kröncke et al., 2003, 0.5mm), and S. Pacific (Alongi, 1992, 0.5mm; Smith et al., 2002, 0.3mm; Palma et al., 2005). Note: reference is followed by the sieve size and color scheme is the same as Figure 22.

The elevated macrofaunal density in submarine canyons, channels, and trenches has been reported by many investigators (Rowe et al., 1982; Gage and Tyler, 1991, Vetter and Dayton, 1998). The high sedimentation rate, major river runoff and the funneling effect on the detritus and terrigenous plants enhance the benthic production over the adjacent continental slope area (Gage and Tyler, 1991). This kind of enhancement is especially obvious at the head of submarine canyons. For example, there was a 3 to 4

fold of increase in macrofaunal abundance in MT1 compared to other shelf breaks stations, which led to an apparent faster rate of decline in standing stocks with depth. However, our results suggested that "the macrofaunal stocks decreasing with depth in the canyon is similar to the general pattern of decline outside the canyon" (Rowe 1983). The seeming elevated rate of decline in density in the "canyon" system was due to the net accumulation of organic materials from the Mississippi River and adjacent shallow continental margin, which enhanced the benthic stocks in MT1. Among transects outside of the "canyon" system, the animal density was slightly higher in transect C than in the transect RW, W, and S39-44 (Figure 12), but the rates of decrease were similar. We believe that this might be associated with the closeness of transect C to the Mississippi Canyon and Fan. As a transition between the "canyon" and "normal" slope, transect C might experience higher energy supplies while the horizontal transport of sediments or detritus from the continental shelf and slope into the submarine canyon.

4.3. Biological diversity

Rex (1981) compared four important macrofauna taxa: the gastropods, polychaetes, protobranch bivalves, and cumacean crustaceans in the western N. Atlantic. He concluded that all four groups had peak diversity at intermediate depth (2300-2800m) and the whole macrofaunal community could be characterized by a parabolic pattern along the depth gradient (Rex, 1983). A similar pattern was found in this study, where the richness of α diversity showed a parabolic pattern while the evenness was generally

high and steady across all depths. The most distinct difference of this study from Rex's (1981, 1983) was the shallower diversity maximum in the northern GoM (800-1500m) than in the N. Atlantic (2300-2800m). Since the maximum depth is shallower in the GoM (~3700m) than in the Atlantic (~8600m), both studies suggested a diversity maximum. However, in this earlier study, data were sampled by a combination of epibenthic sleds (Hessler and Sanders, 1967) and anchor dredges (Sanders et al., 1965). These qualitative data are difficult to compare with the present study. In a more recent investigation from the western N. Atlantic, Etter and Grassle (1992) sampled using $0.25m^2$ box cores and 300μm sieve at bathyal depths (250-3029m) along the east coast of the United States. Their results suggested the $E(S_{100})$ was a nonlinear function of depth with peak diversity at intermediate depth. Since the same sampling procedures were used in the DGoMB study, $E(S_{100})$ can be compared among two studies. The models predicted that the maximum $E(S_{100})$ were both 55 species at 1400m, while the shallow minimum $E(S_{100})$ was higher in the northern GoM (45 species) than in the western N. Atlantic (35 species). The deepest data available in Etter and Grassle (1992) was only 2250m, where the $E(S_{100})$ was 45 species compared to 51 species at the same depth of the northern GoM. Although the comparison suggests that the shallow and deepwater values were slightly higher in the DGoMB, the α diversity seems comparable to western N. Atlantic.

The low α and γ diversity on the abyssal plain has been presumed to be the result of energy constraints. Due to the limited amount of energy (food) that is able to reach the sea floor, some species of lower trophic levels can not maintain the critical

density for sustaining viable populations. Consequently, it dissuades the predatory species and leads to a loss of diversity (Rex, 1973). In the analyses of species distribution, only 9% of stenozonal species were found exclusively on the abyssal plain, while the rest were the extensions of a subset of the slope species. SIMPER also suggested that the euryzonal species made the highest contribution to the abyssal zone. This low diversity and low endemism suggests a possible source-sink dynamics (Rex et al., 2005), with a balance between chronic extinction due to energy constraints and immigration from the continental margin regulated and sustained the abyssal populations. Since most deep-sea, non-chemosynthetic polyachaetes and peracarid crustaceans are brooders (Gage and Tyler, 1991; Young, 2003), the prevalence of planktonic, lecitotrophic larvae of protobranch bivalves (Zardus, 2002) were better suitable for examining the source-sink dynamics. The relative abundances of bivalves increased from around 5% at the shelf break to 15% on the abyssal plain, while the contributions to the average similarity of faunal zones also increased from around 10% (Zone 1) on the upper slope to 50% (Zone 4) on the abyssal plain (Figure 8), suggesting that bivalve species were very well adapted to the deep-sea environment. The success of deep-sea bivalves is probably due to the deposit feeding mode and the high gut to body volume ratio. The elongated and coiled gut increases the sediment retention time and allows better conversion and absorption of the labile organic materials (Gage and Tyler, 1991). We also found that 60% of abyssal bivalve species were euryzonal and none were stenozonal species on the abyssal plain; therefore, the dispersal ability of protobranch bivalves may couple with the digestive physiology to facilitated success on the abyssal plain. However,

the density of individual bivalve species in this study was much higher than the density that Rex et al. (2005) reported for the inverse density dependence and Allee effect in the western North Atlantic. The average species density for bivalves in the abyssal GoM was 1.9-11.6 (individuals/m^2) with only one site of 23.2 (individuals/m^2). These are about the number for every 100 m^2 that reported on the abyssal plain of the western North Atlantic (Rex et al., 2005). The difference might due to that the box core (this study) sampled burrowed fauna better than the benthic sled (Rex et al., 2005), but it may also imply that viable reproduction may be possible in the abyssal GoM; thus, we suggested that self sustained reproduction and source-sink dynamics are both important for regulating the faunal composition and species diversity in the abyssal zone.

This is the first time that the study of deep-sea fauna was extended to such a broad horizontal scale. These zonal boundaries would provide a simple, persistent way for the decision making of conservation policy, such as marine protected area or deep-sea gas and oil exploration. This baseline information also creates opportunities for natural experiments, which the ecological processes and community function can be related to the structure and composition in the deep sea (Carney, 2005). The low abyssal diversity has been reported in many deep-sea studies. However, due to remoteness and isolation of the abyssal plain, most deep-sea programs faced the same obstacles that we are using the potentially insufficient samples to represent the species richness on vast area with sparse population density. In the present study, we still know very little about the distribution and composition of the abyssal fauna. The relatively low sampling efforts on the abyssal plain than on the continental margin can potentially underestimate

abyssal diversity. In the future, a combined exploration between the US and Mexico will be essential to understand the spatial and temporal variation of the abyssal GoM.

5. CONCLUSIONS

Based on the results of this study, we can make the following conclusions:

1) Depth (or in fact something correlated with it) is the single most important factor controlling the decreasing stocks, diversity patterns, and species composition.
2) The production and resultant input of organic materials creates an east-west gradient. Although the resolution was not as fine as the depth gradient, a significant east-west difference was observed in species composition.
3) The deep, northern GoM is characterized by four distinct depth dependent faunal zones, two of which are divided horizontally in the middle of the basin.
4) Within the four (plus 2 sub-zones) faunal zones, the benthic standing stocks were affected by the surface productivity and mesoscale eddies, while the biodiversity could be explained by the time-stability (Sanders, 1968), dynamic equilibrium (Huston, 1971), or source-sink hypothesis (Rex et al., 2005).
5) At the scale of the entire northern half of the basin, the high correlation between biodiversity with depth and export POC fluxes suggested declining food supplies with depth as the major driving force of the faunal turnover (zonation or β diversity).

REFERENCES

Alongi, D., 1992. Bathymetric patterns of deep-sea benthic communities from bathyal to abyssal depths in the western South Pacific (Solomon and Coral Seas). Deep-Sea Research, 39(3/4): 549-565.

Asper, V.L., Deuser, W. G., Knauer, G. A., Lohrenz, S. E., 1992. Rapid coupling of sinking particle fluxes between surface and deep ocean waters. Nature, 357: 670-672.

Baguley, J.G., Montagna, P. A., Lee, W., Hyde, L. J., Rowe, G. T., 2006. Spatial and bathymetric trends in Harpacticoida (Copepoda) community structure in the northern Gulf of Mexico deep-sea. Journal of Experimental Marine Biology and Ecology, 330: 327-341.

Balsam, W.L., Beeson, J. P., 2003. Sea-floor sediment distribution in the Gulf of Mexico. Deep-Sea Research I, 50: 1421-1444.

Berger, W.H., Fischer, K., Lai, C., Wu, G., 1988. Ocean carbon flux: maps of primary production and export production. In: Agegian, C.R. (Ed.), Biogeochemical Cycling and Fluxes between the Deep Euphotic Zone and other Oceanic Realms. NOAA, Washington, DC, pp. 131–176.

Betzer, P.R., Showers, W. J., Laws, E. A., Winn, C. D., DiTullio, G. R., Kroopnick, P. M., 1984. Primary production and particle fluxes on a transect of the equator at 153˚W in the Pacific Ocean. Deep-Sea Research, 31: 1-11.

Biggs, D.C., Hu, C., Müller-Karger, F. E., 2006. Spatial and temporal variations in SeaWifs chlorophyll concentration at deep Gulf of Mexico benthos sampling stations. Deep-Sea Research II, in preparation.

Billett, D.S.M., 1991. Deep-sea holothurians. Oceanography and Marine Biology: an Annual Review, 29: 259-317.

Boland, G.M., Rowe, G. T., 1991. Deep-sea benthic sampling with the GOMEX box corer. Limnology and Oceanography, 36: 1015-1020.

Borowski, C., Thiel, H., 1998. Deep-sea macrofaunal impacts of a large-scale physical

disturbance experiment in the Southeast Pacific. Deep-Sea Research I, 45: 55-81.

Borowski, C., 2001. Physically disturbed deep-sea macrofauna in the Peru Basin, southeast Pacific, revisited 7 years after the experimental impact. Deep-Sea Research I, 48: 3809-3839.

Bray, J.R., Curtis, J. T., 1957. An ordination of the upland forest communities of Southern Wisconsin. Ecological Monographs, 27: 325-349.

Bryant, W.R., Lugo, J., Cordova, C., Salvador, A., 1991. Physiography and bathymetry. In: A. Salvador (Editor), The Gulf of Mexico basin. The geology of North America. Geological Society of America, Boulder, Co, pp. 13-30.

Bryant, W.R., Dellapenna, T., Silva, A., Dunlap, W., Bean, D., 2000. Mega-furrows on the continental rise south of the Sigsbee Escarpment,, AAPG Annual Meeting:, New Orleans, LA.

Burnham, K.P., Overton, W. S., 1978. Estimation of the size of a closed population when capture probabilities vary among animals. Biometrika, 65: 623-633.

Burnham, K.P., Overton, W. S., 1979. Robust estimation of population size when capture probabilities vary among animals. Ecology, 60: 927-923.

Carney, R.S., Carey, A. G., 1976. Distribution pattern of holothurians on the Northeastern Pacific (Oregon, U.S.A.) continental shelf slope, and abyssal plain. Thalassia Jugoslavica, 12(1): 67-74.

Carney, R.S., Haedrich, R. L., Rowe, G. T., 1983. Zonation of fauna in the deep sea. In: G.T. Rowe (Editor), Deep-Sea Biology. The sea, ideas and observations on the progress in the study of the seas. Wily-Interscience, New York, pp. 371-398.

Carney, R.S., 2005. Zonation of deep-sea biota on continental margins. Oceanography and Marine Biology: an Annual Review, 43: 211-279.

Cartes, J.E., Sardà, F., 1993. Zonation of deep-sea decapod fauna in the Catalan Sea (Western Mediterranean). Marine Ecology Progress Series, 94: 27-34.

Cartes, J.E., Jaume, D. Madurell, T., 2003. Local changes in the composition and community structure of suprabenthic peracarid crustaceans on the bathyal

Mediterranean: influence of environmental factors. Marine Biology, 143: 745-758.

Cartes, J.E., Carrassón, M., 2004. Influence of trophic variables on the depth-range distributions and zonation rates of deep-sea megafauna: the case of the Western Mediterranean assemblages. Deep-Sea Research I, 51: 263-279.

Chao, A., 1984. Non-parametric estimation of the number in a population. Scandinavian Journal of Statistics, 11: 265-270.

Chao, A., 1987. Estimating the population size for capture-recapture data with unequal catchability. Biometrics, 43: 783-791.

Chao, A., Hwang, W., Chen, Y. Kuo, T., 2000. Estimating the number of share species in two communities. Statistica Sinica, 10: 227-246.

Chazdon, R.L., Colwell, R. K., Denslow, J. S., Guariguata, M. R., 1998. Statistical methods for estimating species richness of woody regeneration in primary and secondary rain forest of NE Costa Rica. In: F. Dallmeier, Comiskey, J. A. (Editors), Forest biodiversity research, monitoring and modeling: Conceptual background and Old World case studies. Parthenon Publishing, Paris, 285-309.

Christensen, J.P., 2000. A relationship between deep-sea benthic oxygen demand and oceanic primary production. Oceanologica Acta, 23: 65-82.

Clarke, K.R., Warwick, R. M., 2001. Change in marine communities: an approach to statistical analysis and interpretation. PRIMER-E, Plymouth, UK.

Clarke, K.R., Gorley, R. N., 2006. PRIMER v6: User manual/tutorial. PRIMER-E, Plymouth, UK.

Coleman, J.M., Prior, D. B., 1988. Mass wasting on continental margins. Annual Review of Earth and Planetary Sciences, 16: 101-119.

Cutler, E., 1975. Zoogeographic barrier on the continental slope off Cape Lookout, North Carolina. Deep-Sea Research, 22: 893-901.

Day, D.S., Pearcy, W. G., 1968. Species association of benthic fishes on the continental shelf and slope off Oregon. Journal of Fisheries Research Board of Canada,

25(12): 2665-2675.

Ekman, S., 1953. Zoogeography of the sea. Sidgwick and Jackson, London.

Etter, R.J., Grassle, J. F., 1992. Patterns of species diversity in the deep sea as a function of sediment particle size diversity. Nature, 360: 576-578.

Flach, E., Muthumbi, A., Heip C., 2002. Meiofauna and macrofauna community structure in relation to sediment composition at Iberian margin compared to the Goban Spur (NE Atlantic). Progress in Oceanography, 52: 433-457.

Gage, J.D., Pearson, M., Billett, D. S. M., Clark, A. M., Jensen, M., Paterson, G.J. L., Tyler, P. A., 1984. Echinoderm zonation in the Rockall Trough (NE Atlantic). In: B.F. Keegan, O'Connor, B. D. S. (Editors), Proceedings of the Fifth International Echinoderm Conference, Galway., Balkema, Rotterdam, 31-36.

Gage, J.D., 1986. The benthic fauna of the Rockall Trough-regional distribution and bathymetric zonation. Proceedings of the Royal Society of Edinburgh Section B-Biological Science, 88: 159-174.

Gage, J.D., Tyler, P. A., 1991. Deep-sea biology: a natural history of organisms at the deep-sea floor. Cambridge University Press, Cambridge.

Gage, J.D., Lamont, P. A., Tyler, P. A., 1995. Deep-sea macrobenthic communities at contrasting sites off Portugal, preliminary results: I Introduction and diversity comparisons. Internationale Revue der Gesamten Hydrobiologie, 80(2): 235-250.

Gage, J.D., Lamont, P. A., Kroeger, K., Paterson, G. L., Vecino J. L. G., 2000. Patterns in deep-sea macrobenthos at the continental margin: standing crop, diversity and faunal change on the continental slope off Scotland. Hydrobiologia, 440: 261-271.

Gage, J.D., Hughes, D. J., Vecino, J. L. G., 2002. Sieve size influence in estimating biomass, abundance and diversity in samples of deep-sea macrobenthos. Marine Ecology Progress Series, 225: 97-107.

Galéron, J., Sibute, M., Mahaut, M., Dinet. A., 2000. Variation in structure and biomass of the benthic communities at three contrasting sites in the tropical Northeast Atlantic. Marine Ecology Progress Series, 197: 121-137.

Gardner, W., 1989. Baltimore Canyon as a modern conduit of sediment to the deep sea. Deep-Sea Research, 36(3): 323-358.

Grassle, J.F., Sanders, H. L., Hessler, R. R., Rowe, G. T., McLellan, T., 1975. Pattern and zonation: a study of bathyal megafauna using the research submersible Alvin. Deep-Sea Research, 22: 457-481.

Grassle, J.F., Sanders, H. L., Smith, W. K., 1979. Faunal changes with depth in the deep-sea benthos. Ambio Special Report, 6: 47-50.

Grassle, J.F., Morse-Porteous, L. S., 1987. Macrofaunal colonization of disturbed deep-sea environments and the structure of the deep-sea benthic communities. Deep-Sea Research, 34(12): 1911-1950.

Gray, J.S., 1974. Animal-sediment relationships. Oceanography and Marine Biology: an Annual Review, 12: 223-261.

Haedrich, R.L., Rowe, G. T., Polloni, P. T., 1975. Zonation and faunal composition of epibenthic populations on the continental slope south of New England. Journal of Marine Research, 33: 191-212.

Haedrich, R.L., Rowe, G. T., Polloni, P. T., 1980. The megabenthic fauna in the deep sea south of New England, USA., 57: 165-179.

Hamilton, P., 1990. Deep currents in the Gulf of Mexico. Journal of Physical Oceanography, 20: 1087-1104.

Hamilton, P., Lugo-Fernandez, A., 2001. Observations of high speed deep currents in the northern Gulf of Mexico. Geophysical Research Letters, 28(14): 2867-2870.

Hecker, B., 1990. Variation in megafaunal assemblage on the continental margin south of New England. Deep-Sea Research, 37: 37-57.

Hessler, R.R., Sanders, H. L., 1967. Faunal diversity in the deep-sea. Deep-Sea Research, 14: 65-78.

Hessler, R.R., Jumars, P., 1974. Abyssal community analysis from replicate box cores in the central North Pacific., 21: 185-209.

Hurlbert, S.H., 1971. The nonconcept of species diversity: a critique and alternative

parameters. Ecology, 52: 577–586.

Howell, K.L., Billett, D. S. M., Tyler, P. A., 2002. Depth-related distribution and abundance of seastars (Echinodermata: Asteroidea) in the Porcupine Seabight and Porcupine Abyssal Plain, N. E. Atlantic. Deep-Sea Research I, 49: 1901-1920.

Huston, M.A., 1979. A general hypothesis of species diversity. The American Naturalist, 113: 81-99.

Hyland, J., Baptiste, E., Campbell, J., Kennedy, J., Kropp, R., Williams, S., 1991. Macrofaunal communities of the Santa Maria Basin on the California outer continental shelf and slope. Marine Ecology Progress Series, 78: 147-161.

Inman, D.L., Nordstrom, C. E., Flick, R. E., 1976. Currents in submarine canyons: an air-sea-land interaction. Annual Review of Fluid Mechanics, 8: 275-310.

Jacob, W., McClatchie, S., Probert, P. K., R. J. Hurst, R. J., 1998. Demersal fish assemblages off southern New Zealand in relation to depth and temperature. Deep-Sea Research I, 45: 2119-2155.

Jochens, A. E., DiMarco, S. F., 2006. Physical oceanography of the deepwater Gulf of Mexico. Deep-Sea Research II, in preparation.

Joint, I., Groom, S. B., 2000. Estimation of phytoplankton production from space: current status and future potential of satellite remote sensing. Journal of Experimental Marine Biology and Ecology, 250: 233-255.

Kröncke, I., Türkay., M., Fiege, D., 2003. Macrofauna communities in the eastern Mediterranean deep sea. Marine Ecology, 24(3): 193-216.

Levin, L.A., Etter, R. J., Rex, M. A., Gooday, A. J., Smith, C. R., Pinda, J. Stuart, C. T., Hessler, R. R., Pawson, D., 2001. Environmental influences on regional deep-sea species diversity. Annual Review of Ecology and Systematic, 32: 51-93.

Magurran, A.E., 2004. Measuring biological diversity. Blackwell.

Markle, D.F., Musick, J. A., 1974. Benthic-slope fishes found at 900m depth along a transect in the Western N. Atlantic Ocean. Marine Biology, 26: 225-233.

Martin, J.H., Knauer, G. A., Karl, D. M., Broenkow, W. W., 1987. VERTEX: carbon

cycling in the northeast Pacific. Deep-Sea Research, 34: 267-285.

Menzies, R.J., George, R. Y., Rowe, G. T., 1973. Abyssal environment and ecology of the world ocean. Wiley, New York.

Moranta, J., Srefanescu, C., Massuti, E., Morales-Nin, B., Lloris, D., 1998. Fish community structure and depth-related trends on the continental slope of the Balearic Islands (Algerian basin, western Mediterranean). Marine Ecology Progress Series, 171: 247-259.

Murray, J., 1895. General observation on the distribution of marine organisms. Report on the scientific results of the voyage of H.M.S. Challenger during the years 1873-76, Summary of Scientific Results, 2: 1431-1462.

Nunnally, C.C., 2003. Macrobenthic community structure and total sediment respiration at cold hydrocarbon seeps in the northern Gulf of Mexico. M. S. Thesis, Texas A&M University, College Station.

Ohta, S., 1983. Photographic census of large-sized benthic organisms in the bathyal zone of Suruga Bay, central Japan. Bulletin of the Ocean Research Institute, 15: 1-244.

Okey, T.A., 1997. Sediment flushing observations, earthquake slumping, and benthic community changes in Monterey Canyon head. Continental Shelf Research, 17(8): 877-897.

Olabarria, C., 2005. Patterns of bathymetric zonation of bivalves in the Porcupine Seabight and adjacent Abyssal plain, NE Atlantic. Deep-Sea Research I, 52: 15-31.

Palma, M., Quiroga, E., Gallardo, V. A., Arntz, W., Gerdes, D., Schneider, W., Hebbeln, D., 2005. Macrobenthic animal assemblages of the continental margin off Chile (22° to 42°S). Journal of the Marine Biological Association of the UK, 85: 233-245.

Palmer, M.W., 1991. Estimating species richness: the second-order Jacknife reconsidered. Ecology, 72: 1512-1513.

Pearcy, W.G., Stein, D., Carney, R. S., 1982. The deep-sea benthic fish fauna of the north-eastern Pacific Ocean on Cascadia and Tufts Abyssal Plains and adjoining

continental slopes. Biological Oceanography, 1: 375-482.

Pequegnat, W.E., Gallaway, B. J., and Pequegnat, L. H, 1990. Aspects of the ecology of the deep-water fauna of the Gulf of Mexico. American Zoologist, 30: 45-64.

Powell, S.M., Haedrich, R. L., McEachran, J. D., 2003. The deep-sea demersal fish fauna of the northern Gulf of Mexico. Journal of Northwest Atlantic Fishery Science, 31: 19-33.

Puig, P., Ogston, A. S., Mullenbach, B. L., Nittrouer, C. A., Parsons, J. D., Sternberg, R. W., 2004. Strom-induced sediment gravity flows at the head of the Eel Submarine Canyon, Northern California Margins. Journal of Geophysical Research, 109(C03019): 1-10.

Rex, M.A., 1973. Deep-sea species diversity: decrease gastropod diversity at abyssal depths. Science, 181: 1051-1052.

Rex, M.A., 1977. Zonation in deep-sea gastropods: the importance of biological interactions to rates of zonation. In: B.F. Keegan, Ceidigh, P. O., Boaden, P. J. S. (Editors), Biology of benthic organism. Pergamon Press, New York, pp. 521-530.

Rex, M.A., 1981. Community structure in the deep-sea benthos. Annual Review of Ecology and Systematic, 12: 331-353.

Rex, M.A., 1983. Geographic patterns of species diversity in the deep-sea benthos. In: G.T. Rowe (Editor), Deep-sea biology. The sea, ideas and observations on the progress in the study of the seas. Wily-Interscience, New York, pp. 453-472.

Rex, M.A., Stuart, C. T., Etter, R. J., 1997. Large-scale patterns of biodiversity in the deep-sea benthos. In: R.F.G. Ormond, Gage, J. D., Angel, M. V. (Editors), Marine biodiversity: patterns and process. Cambridge University Press, Cambridge, UK, pp. 99-121.

Rex, M.A., McClain, C. R., Johnson, N. A., Etter, R. J., Allen, J. A., Bouchet, P., Warén, A. , 2005. A source-sink hypothesis for abyssal biodiversity. The American Naturalist, 165: 163-178.

Rice, A.L., Thurston, M. H., New, A. L., 1990. Dense aggregations of hexactinellid sponge, *Pheronema carpenteri*, in the Procupine Seabight (northeast Atlantic

Ocean), and possible causes. Progress in Oceanography, 24: 179-196.

Rowe, G.T., Menzies, R. J., 1969. Zonation of large benthic invertebrate in the deep-sea off Carolinas. Deep-Sea Research, 16: 531-537.

Rowe, G.T., 1971. Benthic biomass in the Pisco, Peru upwelling. Investigacion Pesquera, 35(1): 127-135.

Rowe, G.T., Menzel, D., 1971. Quantitative benthic samples from the deep Gulf of Mexico with some comments on the measurement of deep-sea biomass. Bulletin of Marine Science, 21: 556-566.

Rowe, G.T., Polloni, P. T., Horner, S. G., 1974. Benthic biomass estimates from the northwestern Atlantic Ocean and the northern Gulf of Mexico. Deep-Sea Research, 21: 641-650.

Rowe, G.T., Polloni, P. T., Haedrich, R. L., 1982. The deep-sea macrobenthos on the continental margin of the northwest Atlantic Ocean. Deep-Sea Research, 29(2A): 257-278.

Rowe, G.T., 1983. Biomass and production of deep-sea macrobenthos. In: G.T. Rowe (Editor), Deep-sea biology. The sea, ideas and observations on the progress in the study of the seas. Wily-Interscience, New York, pp. 97-121.

Rowe, G.T., Kennicutt, M. C., 2006. Deepwater program: Northern Gulf of Mexico continental slope habitat and benthic ecology. Final Report (contract 30991), U. S. Department of the Interior, Minerals Management Service, Gulf of Mexico OCS Region, New Orleans, LA, in preparation.

Sanders, H.L., Hessler, R. R., Hampson, G. R., 1965. An introduction to the study of deep-sea benthic faunal assemblages along the Gay Head-Bermuda transect. Deep-Sea Research, 12: 845-867.

Sanders, H.L., 1968. Marine benthic diversity: a comparative study. The American Naturalist, 102(925): 243-282.

Sanders, H.L., Hessler, R. R., 1969. Ecology of the deep-sea benthos. Science, 163: 1419-1424.

Sanders, H.L., Grassle, J. F., 1971. The interactions of diversity, distribution and mode of reproduction among major groupings of deep-sea benthos., The ocean world; proceedings of Joint Oceanographic Assembly, Tokyo, pp. 260-262.

Sanders, H.L., 1977. Evolutionary ecology and the deep-sea benthos. In: C.E. Goulden (Editor), The changing scenes in natural sciences 1776-1976. Academy of Natural Sciences, Philadelphia, pp. 223-243.

Shepard, F.P., Marshall, N. F., MacLoughlin, P. A., 1974. Currents in submarine canyons. Deep-Sea Research, 21: 691-706.

Siebenaller, J., Somero, G. N., 1978. Pressure-adaptive differences in lactate dehydrogenases of congeneric fishes living at different depths. Science, 201: 255-257.

Simpson, E.H., 1949. Measurement of diversity. Nature, 163: 688.

Smith, E.P., van Belle, G., 1984. Nonparametric estimation of species richness. Biometrics, 40: 119-129.

Smith, K.L., Baldwin, R. J., Karl, D. M., Boetius, A., 2002. Benthic community responses to pulses in pelagic food supply: North Pacific Subtropical Gyre. Deep-Sea Research I, 49: 971-990.

Snelgrove, P.V.R., Grassle, J. F., Petrecca, R. F., 1996. Experimental evidence for aging food patches as a factor contributing to high deep-sea macrofaunal diversity. Limnology and Oceanography, 41(4): 605-614.

Somero, G.N., Siebenaller, J. F., Hochachka, P. W., 1983. Biochemical and physiological adaptations of deep-sea animals. In: G.T. Rowe (Editor), Deep-sea biology. The sea, ideas and observations on the progress in the study of the seas. Wiley, New York, pp. 261-330.

Stuart, C.T., Rex, M. A., Etter, R. J. , 2001. Large scale spatial and temporal patterns of deep-sea benthic species diversity. In: P.A. Tyler (Editor), Ecosystems of the world: ecosystems of deep oceans. Elsevier, Amsterdam, 297-313.

Suess, E., 1980. Particulate organic carbon flux in the oceans—surface productivity and oxygen utilization. Nature, 288: 260-263.

Thomson, C.W., 1880. General introduction to the zoological series of reports. Report on the scientific results of the voyage of H.M.S. Challenger during the years 1873-76, Zoology, 1: 1-50.

Tyler, P.A., Zibrowius, H., 1992. Submersible observations of the invertebrate fauna on the continental slope southwest of Ireland (NE Atlantic Ocean). Oceanologica Acta, 15(2): 211-226.

Vetter, E.W., Dayton, P. K., 1998. Macrofaunal communities within and adjacent to a detritus-rich submarine canyon system. Deep-Sea Research I, 45: 25-54.

Vinogradova, N.G., 1962. The vertical distribution of the deep-sea bottom fauna in the abyssal zone of the ocean. Deep-Sea Research, 8: 245-250.

Whittaker, R.H., 1960. Vegetation of the Siskiyou Mountain, Oregon and California. Ecological Monographs, 30: 279-338.

Whittaker, R.H., 1972. Evolution and measurement of species diversity. Taxon, 21: 213-251.

Young, C.M., Tyler, P. A., 1993. Embryos of the deep-sea echinoids *Echinus affinis* require high pressure for development. Limnology and Oceanography, 38: 178-181.

Young, C.M., Tyler, P. A., Gage, J. D., 1996. Vertical distribution correlates with pressure tolerances of early embryos in the deep-sea asteroid *Plutonaster bifrons*. Journal of Marine Biological Association of the United Kingdom, 62: 896-887.

Young, C.M., 2003. Reproduction, development and life-history traits. In: P.A. Tyler (Editor), Ecosystems of the deep ocean. Elsevier Science, Amsterdam, The Netherlands, pp. 381-426.

Zardus, J.D., 2002. Protobranch bivalves. Advances in Marine Biology., 42: 1-65.

VITA

Name: Chih-Lin Wei

Address: Department of Marine Biology, Texas A&M University at Galveston, 5007 Ave U, TX 77551

Email Address: weic@tamug.edu

Education: B S, National Chung-Hsing University, 1999